CHARACTERIZATION AND DEVELOPMENT OF THE M2 MELANOPSIN RETINAL GANGLION CELL IN THE CLM-1 TRANSGENIC MOUSE RETINA

by

Sahira F. Husain

Submitted in partial fulfillment of the requirements
for the degree of Master of Science

at

Dalhousie University
Halifax, Nova Scotia
August 2012

DALHOUSIE UNIVERSITY

CLINICAL VISION SCIENCE PROGRAM

The undersigned hereby certify that they have read and recommend to the Faculty of Graduate Studies for acceptance a thesis entitled "CHARACTERIZATION AND DEVELOPMENT OF THE M2 MELANOPSIN RETINAL GANGLION CELL IN THE CLM-1 TRANSGENIC MOUSE RETINA" by Sahira F. Husain in partial fulfillment of the requirements for the degree of Master of Science.

Dated: August 20, 2012

Supervisor: _____

Readers: _____

_____

_____

DALHOUSIE UNIVERSITY

DATE: August 20, 2012

AUTHOR: Sahira F. Husain

TITLE: CHARACTERIZATION AND DEVELOPMENT OF THE M2 MELANOPSIN RETINAL GANGLION CELL IN THE CLM-1 TRANSGENIC MOUSE RETINA

DEPARTMENT OR SCHOOL: Clinical Vision Science Program

DEGREE: MSc CONVOCATION: October YEAR: 2012

_____

Signature of Author

In beloved memory of my Dadajahn (Aktar Husain Arastu)
and my Nanajahn (Hakim H. Ali).

Dedicated to those who are the beats of my heart: my family.

My parents, Baba (Aslam Husain), my Mamama (Almas Husain) and my sisters, Appa (Saima) and Salmamama (Salma).
Love you hamesha!

Table of Contents

List of Tables

List of Figures

ABSTRACT

Retinal ganglion cells (RGCs) undergo continued maturation after birth. RGC development can be influenced by light, but for most RGCs this requires the development of functional retinal circuits that occurs up to 2 weeks after birth. A subpopulation of RGCs express melanopsin (MRGCs) making them intrinsically photosensitive at birth. I hypothesized that this intrinsic photosensitivity could affect the morphology of MRGCs during the postnatal (PN) developmental period (PN 3 to adult). I took advantage of the Clomeleon-expressing transgenic mouse line that, combined with melanopsin immunohistochemistry, allowed for the systematic identification of the M2 MRGC at different PN periods. The pattern of development of the M2 MRGC, characterized through the analysis of 6 morphological parameters, was similar to that described for other types of RGCs. Thus, despite being intrinsically photosensitive, M2 MRGCs did not show substantial developmental differences from other RGC types.

List of Abbreviations

ANOVA	One-way Analysis of Variance
CNS	Central Nervous System
ChAT	Choline acetyl transferase
CLM-1	Clomeleon 1
CM+/M-IR RGC	Clomeleon-expressing, melanopsin-immunoreactive RGC
E	Embryonic
GABA	Gamma Aminobutyric Acid
GCL	Ganglion Cell Layer
GFP	Green Fluorescent Protein
INL	Inner Nuclear Layer
IPL	Inner Plexiform Layer
ipRGC	Intrinsically Photosensitive RGC
JAM-B	Junctional Adhesion Molecule B
LGN	Lateral Geniculate Nucleus
MRGC	Melanopsin Retinal Ganglion Cells
OPN	Olivary pretectal nucleus
ONL	Outer Nuclear Layer
OPL	Outer Plexiform Layer
PB	Phosphate Buffer
PN	Post-Natal

RPE	Retinal pigment Epithelium
RGC	Retinal Ganglion Cell
SCN	Suprachiasmatic nucleus
SD	Standard Deviation
TDFL	Total Dendritic Field Length
TDL	Total Dendritic Length
YFP	Yellow Fluorescent Protein

ACKNOWLEDGMENTS:

Bismillahir Rahmanir Raheem "In the Name of God, the Compassionate, the Merciful"

First and foremost, I would like to thank God, without whom I would not have had the iman, strength or perseverance to pursue any of this.

The important thing is not so much
that every child should be taught,
as that every child should be given the wish to learn.
John Lubbock

I would like to thank my supervisor, Dr. Bill Baldridge, whose guidance, support and encouragement made this achievement possible. This quote is indeed a reflection of you. I have had many people who've 'taught' me various things in life but you are one of the few who has definitely influenced my passion for learning and new love for research. From my initial rough start to the completion of this work your patience, optimism, and motivation were always present to help me accomplish my goal. I will always remember this and thank-you sincerely.

Luis a.k.a Dr. Melanopsin!! D-O-O-D! When I first found out I was going to be working with a Spanish man I was skeptical, and it was for a good reason!;P I came to the retina lab with the idea that I would work hard, do what I needed to do and let things be where they may. I did not expect to have worked with someone who would end up being my neighbor, close friend and then roommate - all in the time frame of four months!:) From skating and snow ball fights to Halloween parties and random get-togethers (Dumplings anyone?) to sharing cookies and curry puff delights it has been a blast to get to know you and Tanya. Though you left me stranded and are not present for the end, I'm blessed to have made and have two close friends. Muchos gracias for your research insight, and trust to let me continue on with the project!

It was a pleasure to work in the retina lab! Janette, Michelle, Kelly, Spring - thank-you soo very much for making all the cakes, cupcakes, cookies, pies, cheesecakes over the months. The sugar high certainly contributed to the much needed energy to get things done. Also you were all there for whenever I need help with antibody dilution calculations (there was a reason why I stopped taking chemistry), confocal help, or the times I had difficulty during experiments. Thank-you for your insight and support!

To Dr. Xu Wang, who was always pleasant company and helped with my experiments – thank-you! I wish you all the best in Washington!

No experience is ever complete without its trials and tribulations and a thank-you goes out to my fellow students who were there to hear my vents frustrations. To my office buddies, Jill, Sally, Setarah, Stu (when you were here), thank-you for all the quirky times and memories. To Sophie and Sung (we should be the 'S' Club), thanks for being so motivated, and enthusiastic about research. Finally, to my fellow night owls, Ben and Liz, thanks for the company and the late night conversations (YAY! I'm not the only one here!) To Julie, Andrea and Cory, thank-you for helping me out with experiments, reading my discussion, and lending a helpful hand when one was needed.

To my supervisory committee, Dr. Balwantray Chauhan, Dr. Francois Tremblay, Dr. Kevin Duffy, and Karen McMain- thank-you for your patience, guidance and insight to make my defense possible.

Finally a huge recognition goes out to my pillars of strength: my family. To my parents, Mamama and Baba, thank-you for always giving your unconditional love and support and your countless duas. To my sister pisters, Appa (Dr. FPWD) and Salmamama(Daffadookal) thank-you for being my absolute best friends. To Nadia, my sister away from home, thanks for the hangouts and guidance. Love you all!

CHAPTER 1: INTRODUCTION

1.1. The Eye and the Retina

The capacity for vision requires an intricate functional system that begins with the eye. The ocular system is made of multiple components that require systematic organization in order to function properly. These components, from anterior to posterior, include the cornea, the iris, the lens, the retina, and the optic nerve (for review, see Kandel, Schwartz, & Jessell, 2000). The cornea and lens are the refracting elements that focus light rays on the retina. The iris controls the amount of light entering the eye, part of a larger system (adaptation) that maintains visual sensitivity over the wide range ($\sim 10^{12}$) of light intensities encountered in nature. The optic nerve is the conduit by which information is relayed from the retina to the brain (Kandel et al., 2000).

The retina contributes to vision in three ways (for review, see Dowling, 2012). The first is to convert visual images into an electrochemical signal interpretable by the brain. Second, the retina is important for light adaptation. Two types of photoreceptors (rods and cones) are suited for dim or bright light conditions, respectively, and intrinsic network (Dowling, 2012) mechanisms extend the range of adaptation. Third, the circuitry of the retina is involved in various types of neuronal processing that can, depending of the species, form the basis of contrast sensitivity, the foundation for color vision, and contribute to the detection of motion.

The retina is comprised of three cellular layers that are interposed by two synaptic layers. The cellular layers, referred to as nuclear layers, contain the cell bodies or somata of retinal neurons, while the plexiform layers contain the processes where different neurons form synapses with each other. From outer (distal) to inner (proximal) the retina

consists of the following major layers: the retinal pigment epithelium (RPE) layer, the outer nuclear layer (ONL), the outer plexiform layer (OPL), the inner nuclear layer (INL), the inner plexiform layer (IPL), the ganglion cell layer (GCL) and the nerve fibre layer (Dowling, 2012).

Each of the cellular layers contains distinct types of somata. The somata of the photoreceptors lie in ONL. As mentioned above, there are two types of photoreceptors, rods and cones that contain the photopigment and associated molecular machinery to convert light into an electrochemical signal. Rods are active in scotopic (dim light) conditions whereas cones are active during photopic (bright light) conditions and are involved in color vision (for review see Remmington, 2005). In primates and some birds, the retina contains a high-density cone region (no rods are present), the fovea centralis, which provides high acuity vision. Most other vertebrates, including most mammals, lack such a region. Many mammals are nocturnal and have rod-dominated retinas. For example, in mice ~97% of all photoreceptors are rods (average density of 437,000 rods/mm^2 versus 12,400 cones/mm^2) (Jeon, Strettoi, & Masland, 1998). The differential sensitivity of cone types to light of different wavelengths is the basis of color vision. Humans possess three different cone types with peak sensitivities at 420 nm (blue), 531 nm (green) and 588 nm (red) (see Remmington, 2005). In contrast, mice possess only two types of cone photoreceptors, with peak sensitivities near 350 nm (ultraviolet) and 510 nm (blue/green) (Lyubarsky et al., 1999; Nikonov et al., 2006).

In addition to the photoreceptors, there are four major classes of retinal neurons: horizontal cells, bipolar cells, amacrine cells and ganglion cells (Dowling, 2012). Horizontal cell somata lie in the outer margin of the INL, bipolar cell somata in the

middle of the INL, and the somata of amacrine cells near the proximal border of the INL. Ganglion cell somata lie in the GCL, as are the somata of some types of amacrine cells, termed “displaced” amacrine cells. Similarly, small populations of ganglion cells “displaced” to the INL have been found in most vertebrate retinas (Dowling, 2012).

The retinal unit that transmits visual information to the brain consists of photoreceptors, bipolar cells and ganglion cells (Galli Resta et al., 2008). Photons are absorbed by photopigment within photoreceptor outer segments thereby triggering a molecular cascade that ultimately decreases the release of the neurotransmitter glutamate onto bipolar cells dendrites. This influences the release of neurotransmitter (also glutamate) from bipolar cells onto ganglion cell dendrites. The ganglion cells then relay signals to the brain. Horizontal cells and many types of amacrine cells modulate synaptic transmission between photoreceptors and bipolar cells (horizontal cells) and bipolar cells and ganglion cells (amacrine cells) (Remmington, 2005). In mammalian retinas, there are typically 2 anatomical types of horizontal cells, one with an axon, one without. Mammalian horizontal cells receive synaptic input from cones at dendrites but from rods at their axon terminals (Peichl, Sandmann, & Boycott, 1998). Horizontal cells are thought to influence the transmission from photoreceptors to bipolar cells. Similarly, amacrine cells influence bipolar to ganglion cell transmission via the very same processes that are post-synaptic to bipolar cells (Remmington, 2005).

Although there are many morphological types of bipolar cells, there are two physiological types of bipolar cells. ON bipolar cells depolarize in response to light, OFF cells hyperpolarize. Although the mechanism that subserves this is related to the different types of glutamate receptors found on the dendrites of ON and OFF bipolar cells in OPL (for review, see Dowling, 2012), the axon terminals of ON and OFF bipolar cells stratify

in specific parts of the IPL. The axon terminals of ON bipolar cells stratify within the inner (proximal) part of the IPL (called sublamina b), the terminals of OFF bipolar cells stratify within the outer (distal) part of the IPL (sublamina a). Within these sublaminae are also found the dendrites of the ganglion cells that receive synaptic input from each physiological type of bipolar cell. Consequently, ON ganglion cells (that show increased action potential firing rate, or spiking, in response to light) have dendrites in sublamina b of the IPL and OFF ganglion cells (that show decreased spiking in response to light) have dendrites in sublamina a of the IPL. Ganglion cells with dendrites in both sublamina a and b (bistratified cells) are ON-OFF cells, cells that respond with a transient period of increased spiking both at the onset and offset of light.

As mentioned above, synaptic transmission from vertebrate photoreceptors to the brain involves a chain of three neurons. However, the actual circuit in the mammalian retina depends on light level and the type of photoreceptors involved. Under well-lit (photopic) conditions the pathway is essentially as described, cones signal bipolar cells, these cone-driven bipolar cells (of which there are multiple morphological types) signal ganglion cells (Leamey, Protti, & Bogdan, 2008). However, under low light (scotopic/ mesopic) conditions, rods signal the rod bipolar cell, of which is there is just one morphological and physiological (ON) type. The rod bipolar cell does not make direct synaptic contact with ganglion cells but instead synapses with the rod (or AII) amacrine cell (Leamey, Protti, & Bogdan, 2008). This amacrine cell makes sign-conserving electrical synapses (gap junctions) with ON cone bipolar cells and sign-inverting glycinergic synapses with OFF cone bipolar cell thereby influences ON and OFF ganglion cells, respectively. Thus, rod bipolar cells, via AII amacrine cells, relay their input to the pre-existing cone pathways.

Along with neurons that are involved in synaptic transmission and form the circuits of the retina, there are glial cells that are present to provide structural and nutrient support. Astrocytes, Müller cells and microglial cells are such cells (Leamey et al., 2008). Astrocytes wrap around blood vessels, thereby contributing to the blood-retina barrier. Astrocytes and Müller cells, the latter being radial glia that extend throughout almost the whole extent of the retina, regulate the extracellular levels of potassium and neurotransmitters (e.g. GABA, glutamate) (Dowling, 2012). Microglial cells are wandering phagocytic cells; they increase during injury or inflammation and are involved in the removal of cellular debris (Remmington, 2005).

1.2. Retinal Ganglion Cells

As described above, retinal ganglion cells (RGCs) relay information from the retina to the brain. As such, their responses represent the final product of retinal processing, encoded in changing trains of action potentials. Input from bipolar cells influences the general response properties of RGCs (ON, OFF, ON-OFF) and there is corresponding morphology specifically the location of ganglion cell dendrites within the IPL. However, this is not a complete description of RGC function or RGC types. Early on, physiologists recognized that rabbit RGCs could be classified as belonging to one of two broad physiological classes (Barlow, Hill, & Levick, 1964). One class of RGCs possessed antagonistic center-surround receptive fields. In these cells, the response was either ON or OFF if a stimulus was presented over the central region of receptive field (termed the centre) and the opposite (OFF or ON, respectively) if the stimulus was presented in a region at the periphery of the receptive field (termed the surround). The extent of the response of a RGC was due to the outcome of an antagonistic interaction

between the two components of the receptive field (centre vs. surround) and, as such, represented a fundamental mechanism for contract detection. Physiological subtypes of ON and OFF cells were also described in the cat retina, with X cells having sustained responses and linear antagonistic centre-surround interactions and Y cells, with transient responses and non-linear centre-surround interactions (Cugell-Enroth & Robson, 1966).

The other class of rabbit RGCs were different in that, possibly in addition to possessing antagonistic centre-surround receptive fields, some additional aspect of a stimulus (e.g. motion or motion in a particular direction), described as a "trigger feature," generated a changes in spiking (Levick, 1967). Cells of this type would be included in another population of cat RGCs, the W-cells (Stone & Fukuda, 1974).

It became apparent that cat X and Y cells often corresponded to existing morphological classes of RGCs based on Golgi stained material, with X cells (small, numerous, narrow receptive-field size) corresponding morphologically to β-cells and Y cells (large, sparse, wider receptive-field size) to α-cells and W cells corresponding to γ- and δ-morphological types (Boycott & Wassle, 1974; Cleland & Levick, 1974; Cugell-Enroth & Robson, 1966). In the cat both X and Y cells project to the thalamus (lateral geniculate nucleus, LGN) whereas some W cells also project to other targets in the brain, including, but not limited to, the superior colliculus (Boycott & Wassle, 1974).

It is not clear to what extent the classification system developed for cat RGCs is applicable to mammalian retinas in general. Nonetheless, it revealed that there are distinct functional and morphological types of RGCs that form parallel channels of visual information sent to the brain. The types of RGCs may differ depending on species, but the concept of functional and morphological groups of RGCs was established.

In the mammalian retina investigators have identified 14-22 different morphological types of RGCs, depending on species and the approach taken (Badea & Nathans, 2004; Dowling, 2012). In the mouse, RGCs have been categorized based on criteria including the soma size and dendritic field size (Sun, Li, & He, 2002). Other studies have differentiated cells based on cluster analysis of stratification depth, the dendritic arbour area and dendritic density (Badea & Nathans, 2004; Kong et al., 2005). That each type of RGC in these classification schemes is functionally distinct has not been established, but other approaches provide convincing evidence of unique groups of RGCs. The manipulation of mouse genetics has contributed greatly to such work through the generation of transgenic lines where unique populations of RGCs express markers allowing systematic anatomical and physiological study. For example, in the retinas of mice that were engineered to express yellow fluorescent protein (YFP) under the control of the JAM-B regulatory element (a gene associated with the immunoglobulin superfamily), the complete population of a single morphological and functional type of RGC (dorsal-ventrally projecting asymmetric dendritic fields, preferential response to upward motion) was revealed (Kim et al., 2008). In another mouse line, where green fluorescent protein (GFP) was under the control of the Hb9 promoter, the complete population of another direction-selective RGC was identified (Trenholm et al., 2011). These are just two examples illustrating both the power of such approaches to the study of RGCs, but they also highlight the fact that there exist unique morphological and functional types of RGCs.

1.3. Melanopsin and intrisincally photosensitive cells

A subset of recently discovered RGCs are cells that express the protein melanopsin (Provencio et al., 1998). Melanopsin (M) is a photopigment and its presence in RGCs results in intrinsic (not requiring rods or cones) photosensitivity (Berson, Dunn, & Takao, 2002; Hattar et al., 2002). Melanopsin RGCs (MRGCs) have subsequently been found to play important roles in non-visual photic signalling, including the entrainment of circadian rhythm and the pupillary light reflex, associated with their projections to the suprachiasmatic nucleus (SCN) and olivary pretectal nucleus (OPN), respectively (Gooley et al., 2001; Hannibal et al., 2002; Hattar et al., 2003; Lucas et al., 2003). In rodents MRGCs make up 1-3% of the entire RGC population (Hattar et al., 2002) and, though initially thought to constitute a single type, ultimately more than one type of MRGC was described (Do & Yau, 2010; Schmidt, Chen, & Hattar, 2011).

MRGCs are unique in that they can respond to light in the absence of rod and cone photoreceptors (Schmidt & Kofuji, 2010). Nonetheless, like conventional RGCs, MRGCs receive synaptic input from bipolar cells. Cones have been found to have the greatest influence on MRGCs, although there is also evidence supporting rod input (Bailes & Lucas, 2010; Schmidt & Kofuji, 2010). Consequently, in mice lacking melanopsin (but without the loss of the RGC type itself) photoentrainment is not lost, although phase shifting (light-induced change in circadian rhythm pattern) was attenuated (Panda et al., 2002). This suggests that, with respect to circadian rhythms, the response of MRGCs, and the signalling of the SCN, is a combination of both synaptic input (from cone and rods) and intrinsic phototransduction. Similarly, in melanopsin knock-out animals, the pupilllary light reflex is attenuated, not abolished (Lucas et al., 2003). Although both rod/cone and melanopsin signalling contribute to photoentrainment and the pupillary light

reflex, the unique contribution of melanopsin is thought to provide sustained, non-adapting responses, in particular to the brightest levels of photopic light (Zhu et al., 2007).

Initial studies (Berson et al., 2002; Hattar et al., 2002) identified just one type of MRGC. This result was based on immunocytochemistry and retrograde labelling from the SCN. With the development of other antibodies, and genetic approaches to express fluorescent protein in MRGC, it has now been confirmed that there are at least four different types of melanopsin cells and perhaps as many as five (Berson, Castrucci, & Provencio, 2010; Müller et al., 2010; Schmidt et al., 2011). One advantage of immunocytochemical analysis of MRGCs is that, as melanopsin is expressed on the soma and on the surface of the dendrites and the axon extending from the cells, immunocytochemistry reveals the entire morphology of the cell (Berson et al., 2010; Hattar et al., 2002)**.**

Initially three types of MRGC were described and identified as M1, M2 and M3 cells. One of the key differences between these cell types was their level of stratification in the IPL. M1 cells stratify in the outer, or OFF sublamina of the IPL (Bailes & Lucas, 2010; Berson et al., 2010; Hattar et al., 2006; Müller et al., 2010; Schmidt et al., 2011). M2 cells stratify in the inner or ON layer of the IPL and M3 cells are bistratified, thus they have dendrites extending into both the outer (OFF) and inner (ON) laminae of the IPL (Bailes & Lucas, 2010; Berson et al., 2010; Müller et al., 2010; Schmidt et al., 2011). Other distinguishing features of the cells include their soma size, dendritic field size, and the shape of the dendritic arbour. M1 cells have a smaller soma and dendritic field diameter in comparison to M2 cells (Berson et al., 2010). In addition, M2 cells have radiating dendrites and a highly branched dendritic arbour. M3 cells are larger than the

former two. Their dendritic arbours, within both sublaminae of the IPL, are similar to M2 cells but there is variability in the proportion of dendrites that stratify in the outer and inner laminae of the IPL (Berson et al., 2010; Schmidt et al., 2011).

Recently, two new subtypes of MRGCs were described and assigned the designations M4 and M5. Ecker et al. (2010) found that these cells were not immunoreactive to the melanopsin antibodies used previously hence they were identified via a transgenic mouse line in which a fluorescent protein expression was driven by the melanopsin gene (OPN4) promoter. These cells both stratified in the inner (ON) lamina of the IPL. M4 cells have similar characteristics to M2 cells: a large soma and a large radially branching dendritic arbour. In fact, aside from immunoreactive properties, the measure of the total dendritic length is the only way to distinguish between M2 and M4 cells. In contrast, soma sizes of the M5 cells are quite small and their dendritic arbour had a more condensed and bushy appearance. Despite the morphological differences between the 4 or 5 types of MRGCs, physiological differences between each cell type are detectable but generally modest (Schmidt et al., 2011). It is also not clear if different types of MRGCs project to specific regions of the brain. For example, it is known that M1 cells project to both the SCN and the OPN (Schmidt et al., 2011).

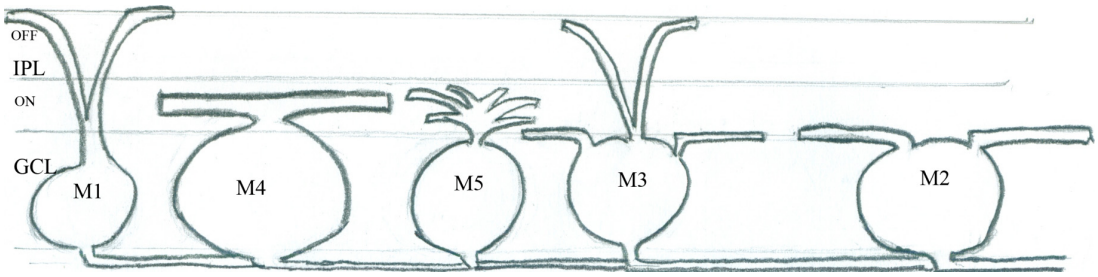

Figure 1: The MRGC subtypes differ in morphology and their level of dendritic stratification. M1 cells stratify in the off (sublamina a) division of the IPL whereas M2, M4 and M5 stratify in the on (sublamina b) division of the IPL. The M3 is a bistratified cell with dendrites in both the on and off sublaminas of the IPL. Modified from Schmidt et al. (2011).

1.4. Retinal Ganglion Cell Development

All of the neurons of the retina develop from neuroepithelial progenitor cells of the optic cup (Napier & Link, 2009). RGCs are the first to differentiate and do so beginning at embryonic day (E) 12 and ending shortly after birth (Wingate & Thompson, 1994; Zhang, Fu, & Barnstable, 2002). Once RGC differentiation occurs, growth of RGC axons and dendrite formation is first dependent on several intrinsic and extrinsic factors. For instance, extracellular factors, such as, peptide trophic factors, and cell adhesion molecules, are required for appropriate dendritic and axon growth (Goldberg et al., 2002). Transcription factors, such as Brn3b, play an important role in axonal extension and dendrite formation (Goldberg, 2008; Napier & Link, 2009). Brn3b is crucial for cellular development; without this transcription factor, 80% of RGCs die prior to birth (Goldberg, 2008). Unlike axonal growth, dendritic growth is dependent mostly on extrinsic retinal cues (Goldberg, 2008).

The development of mammalian RGC cells continues after birth. Notable is that approximately 50% of RGCs undergo apoptosis, or programmed cell death, during this period (in mouse up to postnatal day (PN) 11 but peaking at PN 2 – PN 5) (Young, 1984; Zhang et al., 2002). Several studies have studied the morphology of mouse RGCs during postnatal development. Coombs, Van Der List, & Chalupa, (2007) examined several morphological parameters at different postnatal time points. They concluded that there were three common patterns associated depending on which parameters of RGC morphology were considered. For some parameters (dendrite number, branch angle, symmetry, tortuosity, and axon diameter) there were no changes from the time of birth to adulthood (3 months). A second group of parameters (soma area, dendritic field area, and mean branch length) progressively increased during developmental peaking in the adult. The third set of parameters (total dendrite length, spine density, number of branches, dendrite diameter and highest branch order) underwent an initial period of increase from birth to PN 10 followed by a rapid regression that, by PN 15, stabilized prior to reaching the adult age.

Another study of the morphological development of mouse RGCs examined 12 parameters over the period PN 4 to PN 24 (Qu & Myhr, 2011). Depending on which age a parameter increased most, the parameter was then designated as being part of one of three categories. The first category were those parameters that increased after PN 4, reached a peak at PN 8 and remained stable or decreased after PN 8 (total dendritic length, dendritic density, number of dendritic branches, branch order, and branch angle). The second category consisted of parameters that were initially stable (PN 4-PN 8), reached a peak (PN 16-PN 20) and decreased again (PN 21- PN 24) (dendritic field area, mean internal branch length, mean terminal branch length, and tortuosity). Lastly the third category

consisted of those parameters that were constant from PN4 to PN 24 (soma area, dendrite diameter and symmetry).

In another study of mouse RGCs (Ren et al., 2010) a single parameter was investigated in different RGC types. The dendritic field was analyzed in three morphologically defined RGC subtypes: α-cells, direction-selective (DS) RGCs and conventional RGCs (other than α or DS cells). The dendritic field measurement was correlated with eyeball growth and studied in mice aged PN 0 to adult. For each cell type a different growth pattern was revealed. Three phases of growth were described: initial interstitial growth (PN 0-PN 8), rapid growth (PN 8-PN 13) and finally a reduction phase or decrease in growth (PN 13-adult). All three phases were seen in conventional RGCs. However, in α-cells interstitial growth followed by rapid growth was seen but was not followed by the retraction phase. Direction-selective RGCs showed continual expansion that kept pace with eye maturation.

Each of the three studies of RGC development examined different cell types or parameters. Nonetheless, each described three different patterns: growth that peaks near eye-opening, and is maintained throughout adulthood; growth that peaks near eye-opening but than continues to grow up to adulthood; growth that peaks near eye-opening but then diminishes in the adult.

The three studies of RGC morphology during post natal development all show significant changes prior to eye opening, and prior to bipolar cell input and, therefore, the influence of light (see Diao et al., 2004). Nonetheless, a key feature of post natal RGC development is the formation of synapses with bipolar cells and the stratification and maturation of the dendritic arbour shortly after eye opening (Xu & Tian, 2007). A study which manipulated postnatal visual stimulation in mice through light deprivation showed

a loss of appropriate dendritic stratification, particularly within sublamina a of the IPL (Xu & Tian, 2007). This suggests, therefore, that the emergence of light-sensitive bipolar cells after eye opening has some influence on the aspects of RGC development.

1.5. Development of melanopsin ganglion cells

There are few studies that have examined the development of MRGCs. Schmidt et al. (2008) studied the morphology of mouse MRGCs (engineered to express green fluorescent protein in all types of MRGCs) at three age groups (PN 0-PN 2, PN 5- PN7 and PN 17-PN 24). They examined the stratification depth, the dendritic field size and total dendritic length (TDL). Cells from the two youngest age groups were monostratified and did not appear to yet be segregated into different sublaminae. The dendritic field size and TDL increased linearly with age. In addition, they reported that light-evoked responses of MRGCs were evident as early as the first week of post natal development, although initially the responses were weak. However, by PN 11 the responses of MRGCs had already reached adult-like levels. One limitation of this study was that the investigators could not identify which specific type of MRGCs they were studying during development as GFP was expressed in all type of MRGCs.

More recently, McNeil et al. (2011) examined the neurogenesis, axonal targeting and development of melanopsin cells and the associated development of the pupillary reflex. They found that, similar to conventional RGC development, MRGCs differentiate over the period E 11 to E 14 and that MRGCs that innervate the OPN do so during early postnatal ages (PN 7- PN 14).

1.6. CLM-1 Transgenic mouse

A major handicap to the study of the morphological development of MRGCs has been the lack of a method to systematically study specific subtypes of MRGCs. What is needed is a marker that uniquely labels a single MRGC type so that the cell can be identified and studied at earlier developmental time points.

We have identified a transgenic mouse line (CLM-1) in which the M2 type MRGC expresses the fluorescent protein Clomeleon, driven by the Thy-1 promotor (Berglund, 2006). Clomeleon is a fusion protein, composed in part of cyan flourescent protein (CFP) and yellow fluorescent protein (YFP), and designed to report intracellular chloride concentration (Berglund et al., 2006)**.** Furthermore, expression of Clomeleon has been seen in mice at early ages (PN 2) with stable expression even in two year-old mice.

The CLM-1 mouse line shows Clomeleon expression in several regions of the brain, including but not limited to, cerebellar and dentate gyrus granule cells and in neurons of the hippocampus and amygdala (Berglund et al., 2006). Clomeleon expression in the retina was reported in the CLM-1 mouse line, with many (but not all) types of neurons in the GCL and a few in the INL (Haverkamp et al., 2005). In particular, Clomeleon expression in the CLM-1 mouse line was found in one type of bipolar cell and, consequently, was use to systematically study this retinal neuron (Haverkamp et al., 2005).

Although Clomeleon expression is found in many cell types in the GCL, its expression in just one type of MRGC (M2 cells) allowed us to use it to study the morphology of this cell type in mice of different post natal ages. Studying the post natal development of the mouse M2 MRGC contributes to our overall understanding of mammalian RGC development, providing another specific type to consider and compare

to other RGC types. The intrinsic photosensitivity of MRGCs, even prior to eye opening, also raises the possibility that the pattern of development will be different than conventional RGCs, where the effect of light requires the development of active bipolar cell input after eye opening. In fact, a **guiding hypothesis** of this work is that the pattern of M2 MRGC post natal development will be different than that reported for conventional RGCs.

CHAPTER 2: METHODOLOGY

2.1. Animals

All procedures were conducted according to the guidelines of the Canadian Council on Animal Care and protocols approved by the Dalhousie University Committee on Laboratory Animals. A breeding pair of transgenic CLM-1 mice (where the protein clomeleon is expressed under the control of the Thy-1 promotor; see Berglund et al., 2006), was provided by Dr. George Augustine (Duke University, Durham, NC) and all animals used in the study were derived from the colony established from these original breeders.

2.2. Retina Isolation

Mice were injected with 0.1 ml of Euthansol**,** and then subject to cervical dislocation. The eyes were enucleated and placed in Hibernate-A media (Brain Bits Inc., Springfield, IL). Under a dissecting microscope, the retina was isolated from the eye. First, a hole was made in the cornea, the perimeter of the cornea cut and the cornea removed. The scleral tissue, the anterior portion of the eye, was then cut to form an eyecup, and the lens extracted. The retina was then gently peeled from the eyecup and placed in Hibernate-A.

To permit flattening of the retina, radial incisions were made at each quadrant. The retina was then transferred onto a slide with the photoreceptor layer uppermost. Filter paper (black, Millipore H4575229; Billerica, MA) was placed over the retina, such that

photoreceptor layer adhered to the paper, allowing subsequent manipulation of the retina with the GCL exposed.

2.3. Immunolabeling Procedure

The retina, attached to the filter paper, was placed in 4% paraformaldehyde (PFA; Sigma Chemical Co., Burlington, ON) in 0.1M phosphate buffer (PB) for 15 min and then washed three times in a PB for 30 min each. The retina was then placed in blocking serum and placed in the fridge at 4°C for 24 hours. 10% normal donkey serum solution (Jackson ImmunoResearch Laboratories, West Grove, PA**)** was used, as the host animal of the secondary antibody was donkey. The retina was then incubated in melanopsin antibody (Table 1) in PB containing 0.03% Triton X- 100 (Sigma) solution at 4°C for 5-7 days. The retina was washed in three 30 min wash cycles with PB (90 min total). The retina was then immersed in donkey anti-rabbit secondary antibody, (Table 1) dissolved in PB/Triton- X 100 solution at 4°C overnight. The following day, the retina was washed with PB three times with 30 min cycles. The filter paper with the attached retina was mounted on a glass microscope slide and coverslipped using Vectashield (Vector Lab, Burlington, ON) mounting medium.

Table 1: The specific details regarding the Primary and Secondary Antibodies used in this study

Antibody (Dilution)	**Primary Antibody Number/ Manufacturer**	**Host Animal of Primary Antibody**	**Recognized Antigen of Primary Antibody**	**2° Antibody**	**Secondary (2°) Antibody Number Manufacturer**	**Host Animal of (Dilution)**	**Secondary Antibody Conjugate Dye**
Melanopsin 1:2000	Advanced Targeting systems AB-N38 UF006	Rabbit Polyclonal	15 most N-terminal amino acids of Mouse Melanopsin-Cells	Donkey Anti-Rabbit	Jackson Immuno Research Laboratory 43557	Donkey 1:500	Cy 3

2.4. Microscopy

The prepared slides were examined under a Nikon Eclipse E800 Confocal Microscope (Nikon Canada, Mississauga, ON). Confocal micrographs were collected using a Nikon 40X (N.A. 1.40, oil immersion) Plan Fluor objective. An argon 488 nm laser and HeNe 543 nm laser were used to produce blue and green excitation, respectively. This allowed imaging of clomeleon and Cy3, respectively. Stacks of 1 mm thick optical sections (z – axis) were collected for each cell studied.

2.5. Image Analysis

Selected confocal images were further edited and analyzed using Image J **(**rsbweb.nih.gov/ij). Certain morphological parameters, dendritic field size, soma diameter and stratification depth, were measured (see Figure 2 A- C) using EZ C1 software associated with the Nikon confocal microscope. Equivalent soma area was calculated using the formula for the area of an ellipse ($A=\pi ab$) where a and b are the major and minor axis, respectively. The equivalent circular radius was then calculated from ($A= \pi r^2$) and solving for radius. The complete morphology of M2 cells was traced from Z stacks using Fiji software:
(pacific.mpicbg.de/wiki/index.php/Simple_Neurite_Tracer).
Branch points, total dendritic field length (TDFL) and Sholl analysis were all done using the Fiji software (see Figure 2 D-F).

All data were tested for normality using the Kolmogorov-Smirnov and Shapiro-Wilk tests (Sigma Plot, San Jose, CA). Morphological parameters at different ages were

tested for significance using one-way Analysis of Variance (ANOVA) ($p < 0.05$) followed by Tukey's post-hoc comparison (Prism, GraphPad Software, La Jolla, CA).

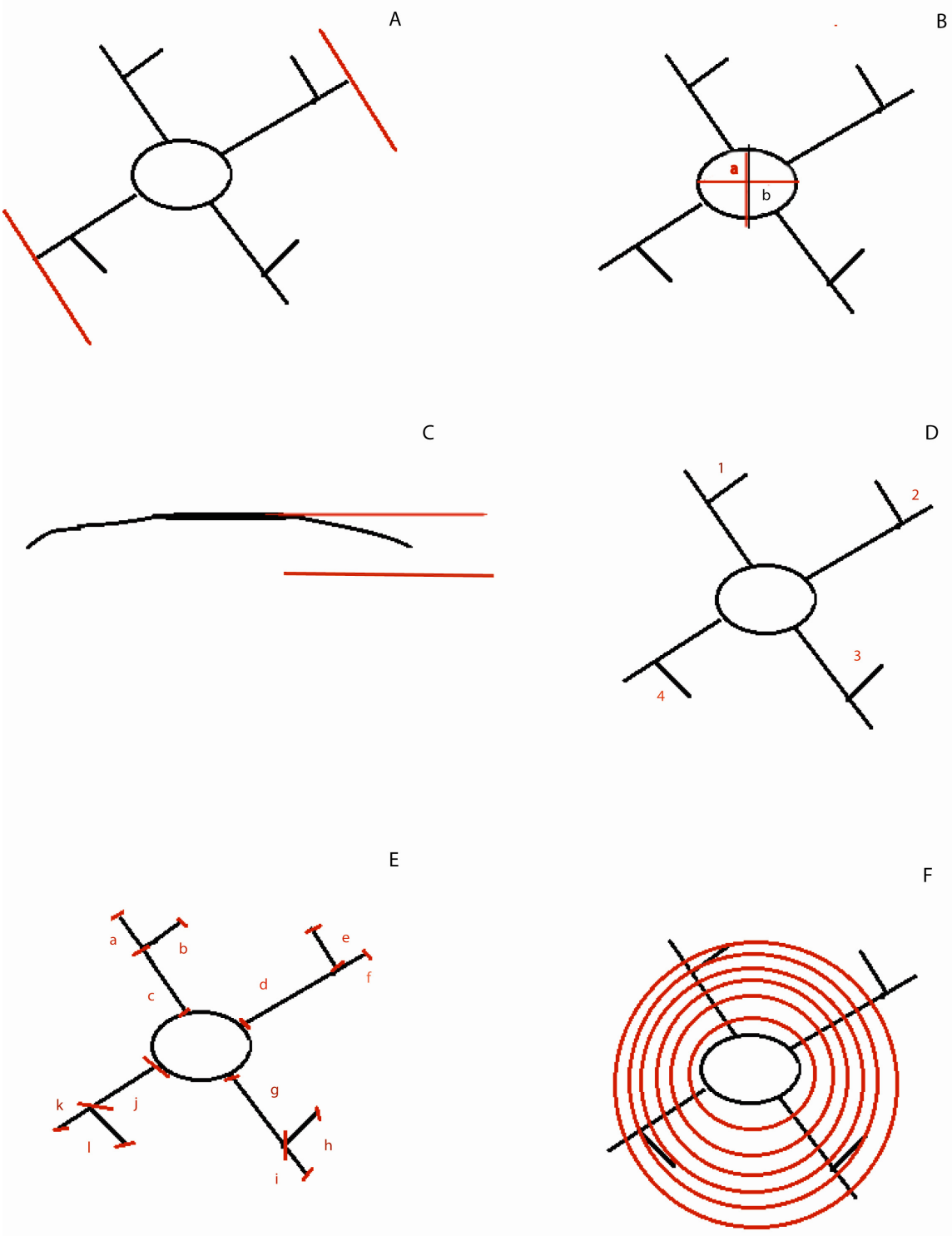

Figure 2: A schematic representation of the morphological parameters studied. (A) Dendritic field size was calculated as the greatest distance separating the tips of dendrites within the plane of the IPL. (B) Soma size (ellipse area and equivalent circular radius) was calculated using the long and short axis (a and b, respectively). (C) Dendritic stratification depth was determined from confocal stacks. (D) Branch point intersections were counted manually. (E) Total dendritic length was calculated from the summation of dendritic line segment lengths (e.g. the sum of line segments a to l). (F) Sholl analysis used concentric rings of fixed thickness and the number of dendrites within each ring counted.

CAHPTER 3: RESULTS

3.1. Some Clomeleon expressing neurons in the GCL are M2 MRGCs

Clomeleon is expressed in a wide variety of neurons in the GCL of the adult CLM-1 mouse (Figure 3A, B). In addition, some cells in the INL also expressed Clomeleon (Figure 3B). The labeling in the INL could represent the population of bipolar cells in the CLM-1 mouse known to express Clomeleon (Haverkamp et al., 2005) or the population of displaced RGCs recently discovered in the CLM-1 retina (Baldridge et al., 2012).

A subpopulation of Clomeleon-expressing RGCS was found to be melanopsin-immunoreactive (Figure 4). As melanopsin is only found in RGCs, these Clomeleon-expressing cells are definitively melanopsin RGCs (MRGCc). The MRGCs that co-localized with Clomeleon had a distinct morphology with monostratified dendrites ramifying in sublamina b of the IPL (Figure 4). By way of comparison, Figure 5 shows two melanopsin immunoreactive ganglion cells that did not express Clomeleon and both had processes that ramified in sublamina a. Comparing Figure 4D and Figure 5D, confirms that the processes of the ganglion cell in Figure 4 ramify in the sublamina b. The cell types illustrated in Figure 5 have morphology typical of M1 MRGCs. Monostratified MRGCs that ramify in sublamina b (Figure 4) of the IPL could be M2, M4 or M5 MRGCs.

Initial morphological analysis of a group of Clomeleon expressing MRGCs (n=18 cells from 6 animals) revealed a population of cells with an equivalent soma size (see Methods) of 19 µm ± 4 µm (mean ± SD), a dendritic field of 268 µm ± 66 µm, 4.5 ± 1.0 primary dendrites and stratification depth (the z-axis distance from the soma to the most distal dendrites within the IPL) of 6.6 µm ± 1.44 µm. Those cells with the best immunolabelling (n=9 cells from 5 retinas) were subjected to further analysis that required detailed tracing of the dendritic tree (an example is shown in Figure 6) that then permitted automated determination of total dendritic length (1454 µm ± 785 µm), the number of dendritic branch points (11 ± 5; n=9) and Sholl analysis (Figure 7) using Fiji software. Sholl analysis provides a metric of dendritic complexity based on the number of dendritic processes that cross at various distances from the soma. In the case of Clomeleon expressing MRGCs the number of crossings reached a maximum of 9 around 80 µm from the soma.

Based on the distinguishing features of M2, M4 and M5 cells (Ecker et al., 2010), these results suggest that the Clomeleon expressing MRGCs are the M2 MRGC type (see Tables 2-6 in Discussion).

3.2. M2 MRGC Morphology During Post Natal Development

Melanopsin-immunoreactive, Clomeleon-expressing neurons in the GCL were identified in mice at six different ages, ranging from PN 3 to adult (PN 31-33), and their morphology examined. A particular focus of this work was post natal development prior to eye opening (around PN 13 in the mouse) to determine if, compared to conventional RGCs, the intrinsic photosensitivity of MRGCs influences the morphology during post natal development prior to the establishment of synaptic input from bipolar cells after eye

opening. An underlying assumption of this work is that this cell type (melanopsin-immunoreactive, Clomeleon-expressing) represents the M2 cell at different developmental time points.

The typical dendritic field of the M2 MRGC is illustrated at each age using representative schematic tracings (Figure 8). To characterize the cells further, six parameters were measured including the size of the dendritic field, the equivalent soma area and radius, the total dendritic length, the number of branch points, and the number of primary dendrites. The extent of dendritic stratification depth (z axis) was also determined. One-way analysis of variance (ANOVA) was used to detect if mean differences in these parameters at different ages were significant statistically. If a given parameter was found to show a statistically significant difference with age, Tukey's multiple comparison test was performed to determine which mean ages were different. As in the case of the analysis of the adult, a larger population of cells was studied in the case of soma size, dendritic field size and primary dendrite number (PN 3, 5 cells from 5 retinas; PN 6, 27 cells from 3 retinas; PN 7, 11 cells from 5 retinas; PN 11, 27 cells from 4 retinas; PN 17, 10 cells from 4 retinas) and the best labeled of these were used for tracing and assessment of total dendritic length, number of branch points, the extent of stratification and Sholl analysis (PN 3, 3 cells from 3 retinas; PN 6, 6 cells from 3 retinas; PN 7, 3 cells from 3 retinas; PN 11, 4 cells from 2 retinas; PN 17, 4 cells from 2 retinas).

Mean dendritic field size did not change significantly over the period PN 3-11 (Figure 9) but was increased after eye opening at PN 17 ($p<0.05$ or better; relative to PN 6, 7 and 11). Mean dendritic field size in the adult (PN 31-33) was significantly larger than mean dendritic field size at the 4 earliest ages studied ($p<0.05$ or better; PN 3-PN

11). Overall this indicates that dendritic field size was relatively constant over the early post natal period but expanded following eye opening.

Mean soma area (or radius) was not changed significantly over the period PN 3-7 (Figure 10) but increased at PN 11 ($p<0.05$; relative to PN 6 and 7) and PN 17 ($p<0.001$; relative to PN 3, 6, 7 and 11). However, soma size/radius was decreased in the adult (PN 31-33) relative to PN 17 ($p<0.001$). This indicates that there was a transient increase in soma area/radius near the time of eye opening followed by a decrease in the adult.

Mean total dendritic field length was not changed significantly over the period PN 3-7 (Figure 11) but was increased at PN 17 ($p< 0.05$ or better; relative to PNs 3, 6, 7). Mean total dendritic field length was decreased in the adult (PN 31-33) relative to PN 17, but this difference was not significant. This suggests that there was a relative increase in total dendritic length following eye opening. There is a trend suggesting that total dendritic field length decreases from after eye opening (PN 17) to adult.

The mean number of branch points was not changed significantly over the period PN 3-11 (Figure 12) but was increased at PN 17 ($p<0.05$ or better; relative to PN 3 and 6). However, mean branch point number decreased in the adult (PN 31- 33) relative to PN 17 ($P<0.05$). This indicates that there is a transient increase in branch point number following eye opening followed by a decrease in the adult.

There was no significant difference between the mean number of primary dendrites (Figure 13) at any age studied.

ANOVA revealed a significant difference ($p=0.03$) in mean dendritic stratification thickness, but the Tukey Multiple Comparison test identified only one specific difference,(Figure 14) between mean dendritic stratification thickness at PN 6 versus PN

11 ($p<0.05$). Overall, these results suggest that there was no systematic difference in stratification thickness over the developmental time periods studied.

Sholl analysis, a measure of dendritic complexity, of the M2 MRGCs at different ages (Figure 15) indicated that the mean peak number of crossings showed no significant change over the period PN 3-11. However, there was a significant increase in the peak number of crossings after eye opening (PN 17) compared to PN 3 ($p<0.05$). A significant increase was also noted between the mean peak number of crossings at PN 11 versus PN 17 ($p<0.05$) but a significant decrease from PN 17 to adult ($p<0.05$). This indicates that the peak number of crossings increases from PN 3 to after eye opening (PN 17) after which there is a decline in the number of crossings in the final adult form.

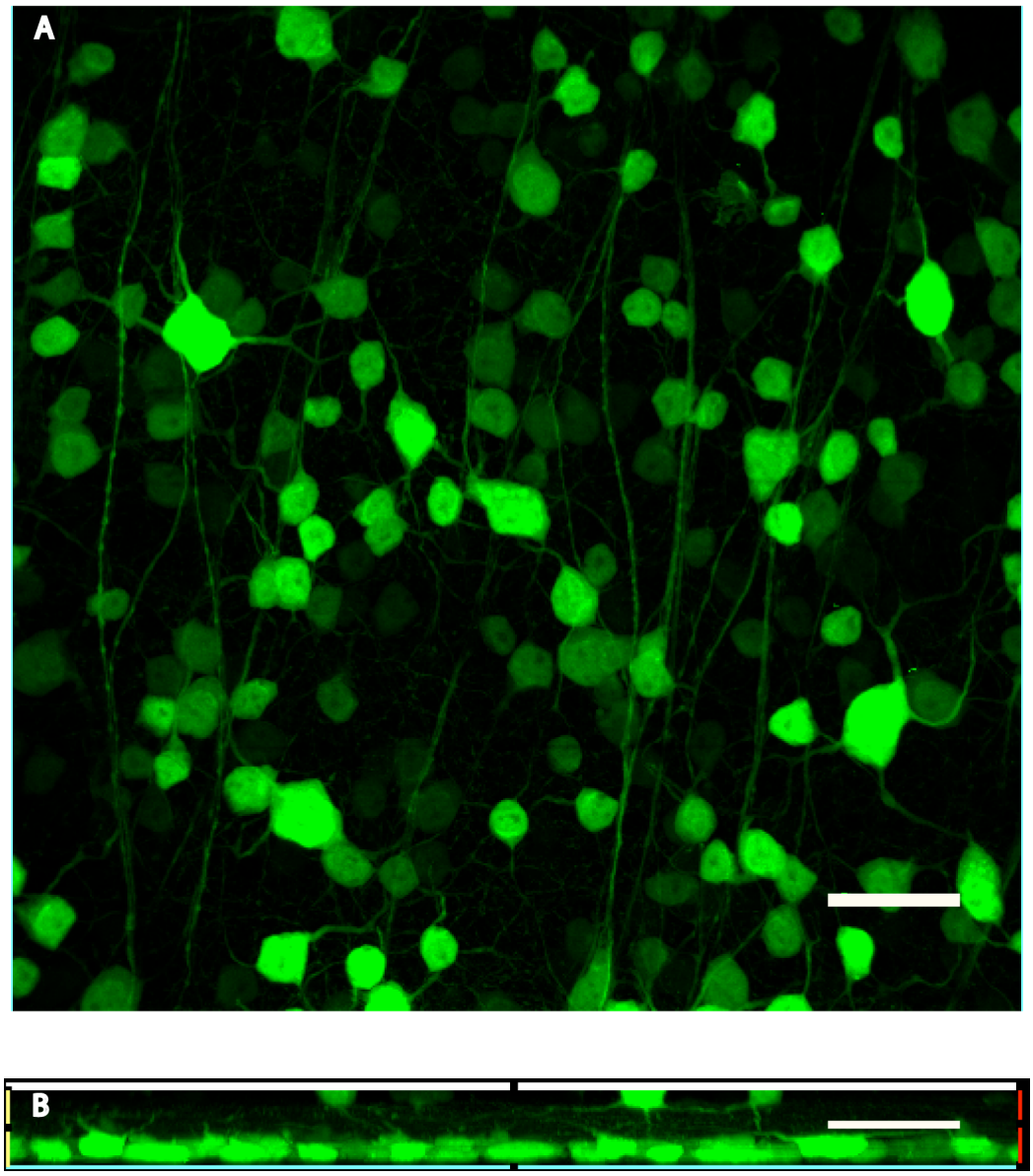

Figure 3: Clomeleon–expressing neurons in the CLM-1 mouse retina. (A) Confocal micrograph of the flat mount view of the GCL illustrating the variety of neurons that express Clomeleon. (B) Confocal orthogonal view illustrating Clomeleon expression in the abundance of cells expressing Clomeleon in the GCL (lower) and a small number of Clomeleon-expressing neurons in the INL. Scale bar = 50 µm.

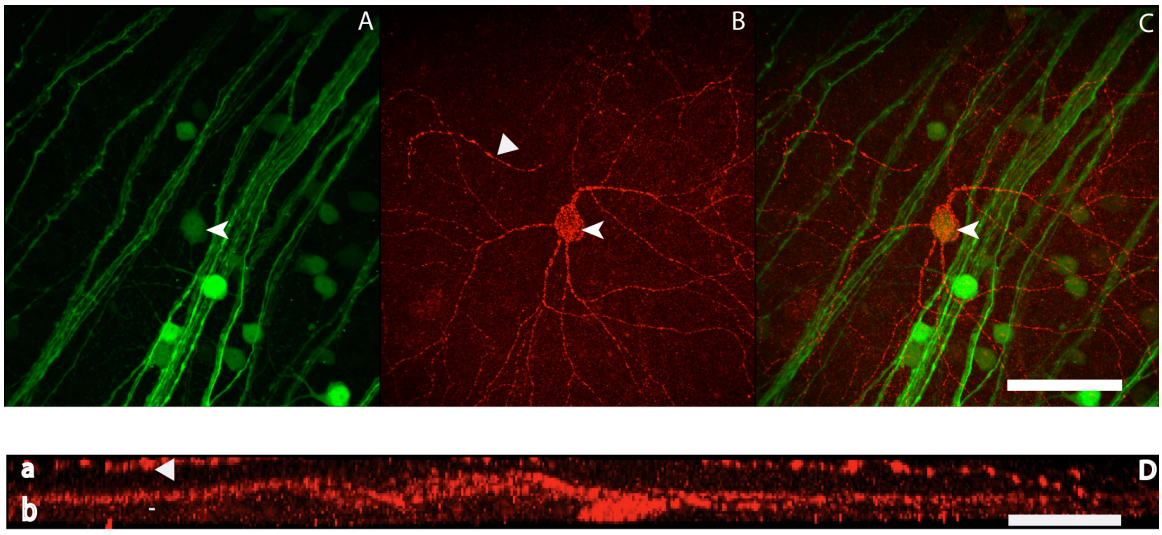

Figure 4: Confocal micrographs of the GCL and IPL in an adult CLM-1 transgenic mouse following melanopsin immunolabeling. (A) Clomeleon expression; (B) Melanopsin immunolabeling; (C) overlay of A and B. A single cell was both Clomeleon-expressing and melanopsin-immunoreactive (see arrow heads in A-C). (D) Orthogonal view of the melanopsin-immunoreactive MRGC (shown in B) that also expressed Clomeleon. Dendritic processes were limited to sublamina b. Note (triangle in B and D) indicating melanopsin-immunoreactive processes that were not associated with the melanopsin-immunoreactive cell (shown in B, arrowhead) and that were located in sublamina a. Scale bar = 50 μm.

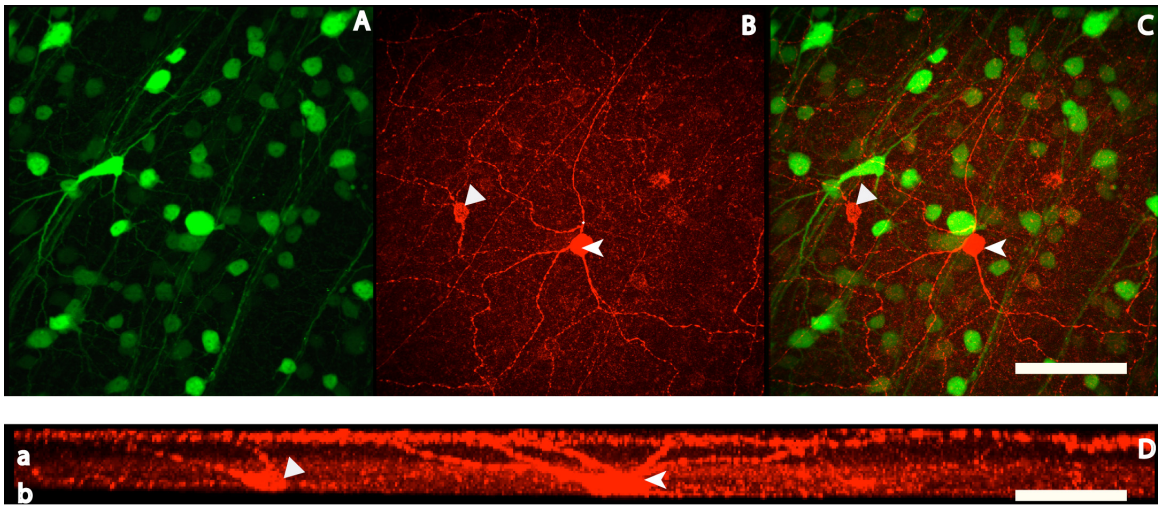

Figure 5: Confocal micrographs of the GCL and IPL in an adult CLM-1 transgenic mouse following melanopsin immunolabeling. (A) Clomeleon expression; (B) Melanopsin immunolabeling; (C) overlay of A and B. Two cells were melanopsin-immunoreactive but did not express Clomeleon (see arrow heads in B and C). (D) Orthogonal view of the melanopsin-immunoreactive MRGC (shown in B). Dendritic processes were limited to sublamina a. Scale bar = 50 μm.

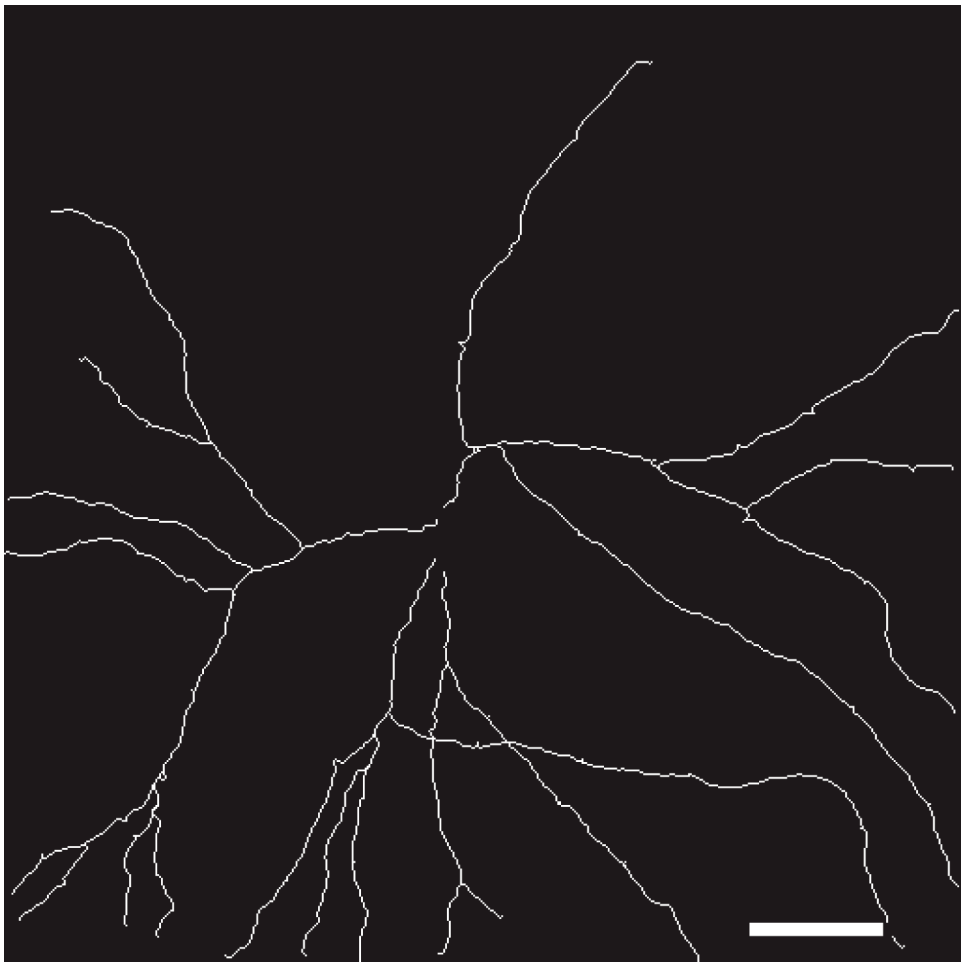

Figure 6: Representative schematic tracing of the dendrites of a Clomeleon-expressing, melanopsin-immunoreactive M2 MRGC from an adult CLM-1 mouse retina. Scale bar = 50 μm.

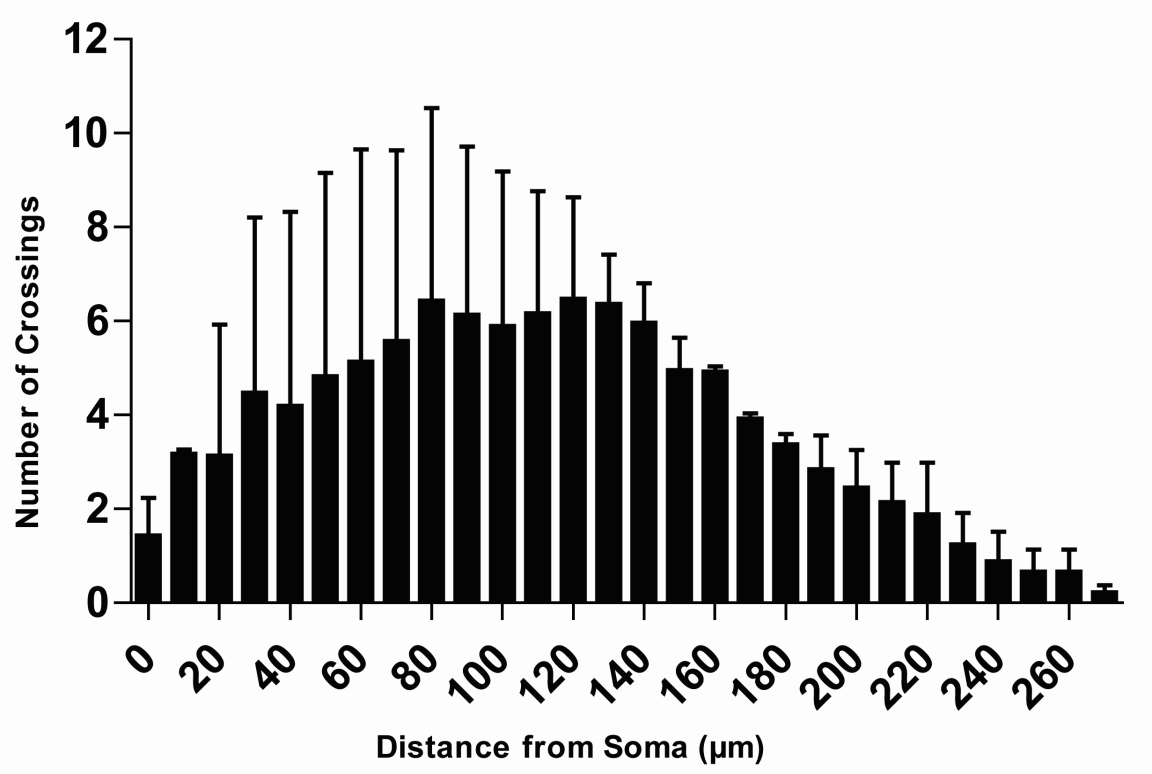

Figure 7: Plot of Sholl analysis of the dendrites of a Clomeleon-expressing, melanopsin-immunoreactive M2 MRGCs from adult CLM-1 mouse retina. Each bin represents a circular region a given distance from the soma; the ordinate indicates the mean (± SD) number of dendrites found crossing each circular region.

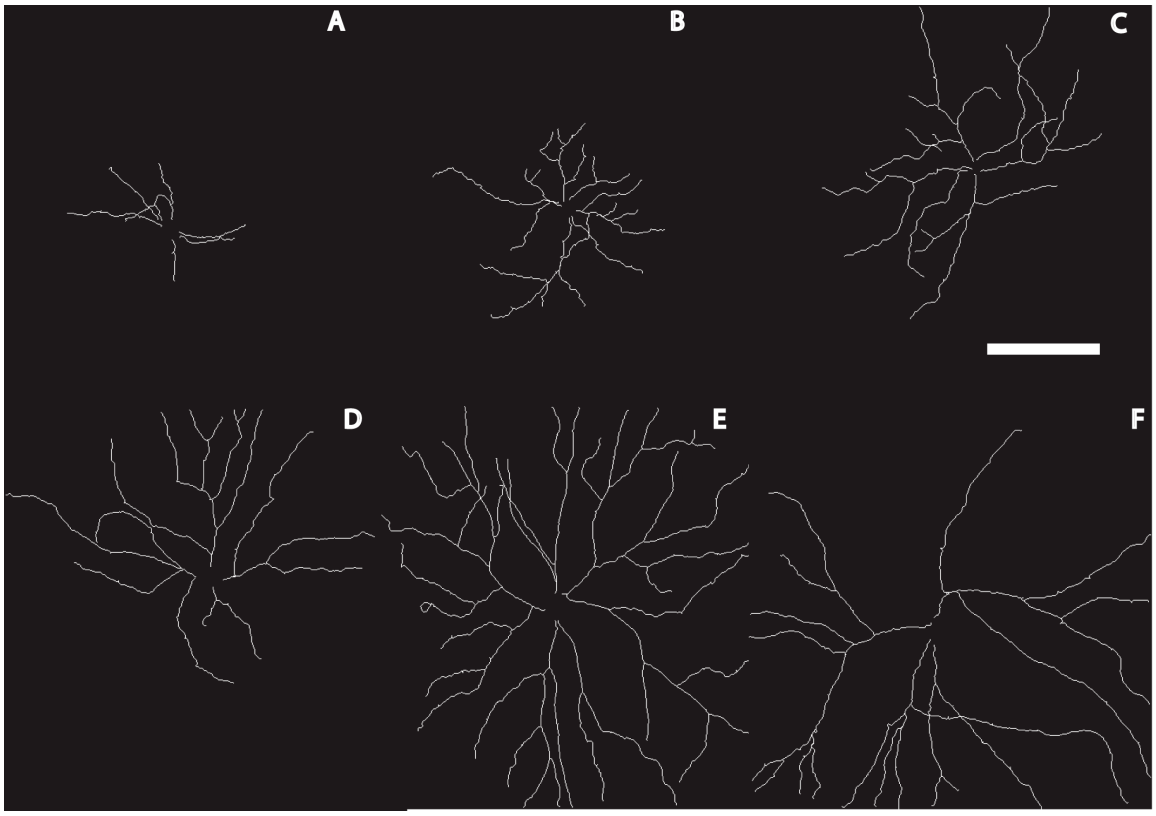

Figure 8: Representative tracings of the dendrites of M2 MRGCs at different ages in the CLM-1 mouse. (A) postnatal age (PN)3, (B) PN 6, (C) PN 7, (D) PN 11, (E) PN 17, and (F) PN 31-33. Scale bar = 50 µm.

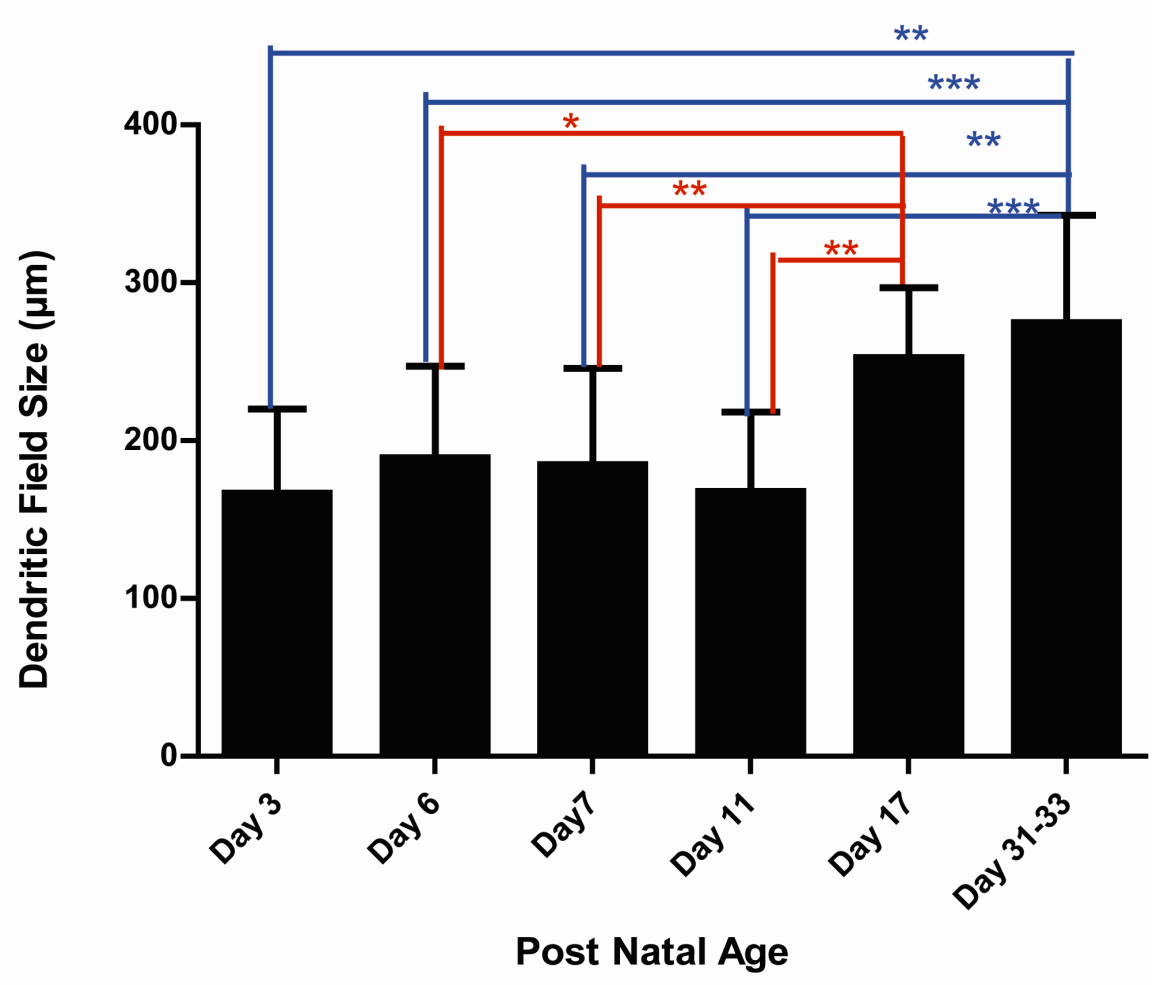

Figure 9: Plot of mean (± SD) dendritic field size of M2 MRGCs at 6 developmental time period (PN 3- PN 31/33). Asterisks indicate significance of Tukey analysis following ANOVA: *p<0.05; **p<0.01; ***p<0.001.

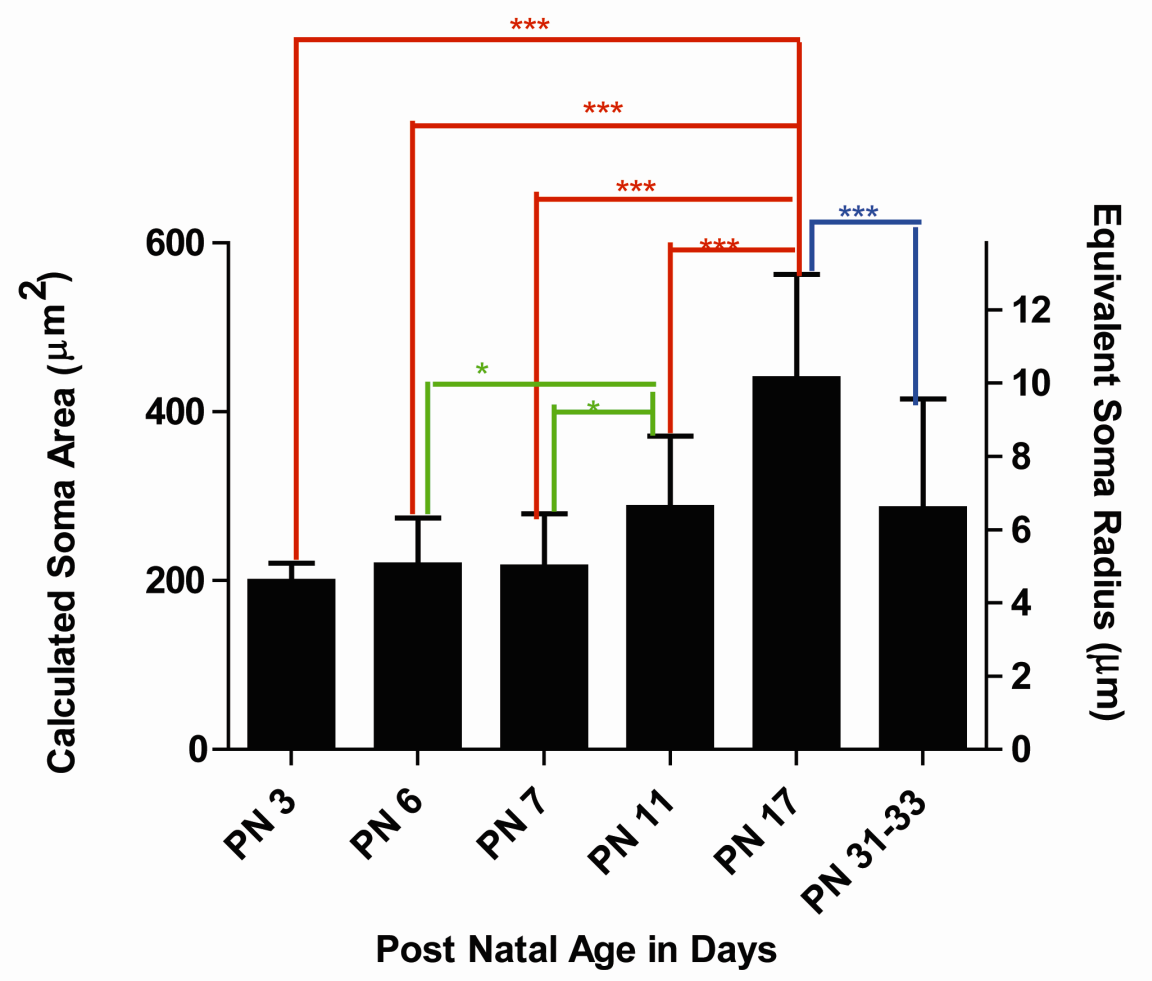

Figure 10: Plot of mean (± SD) M2 MRGC calculated soma area and equivalent soma radius (PN 3- PN 31/33). Asterisks indicate significance of Tukey analysis following ANOVA: *p<0.05; ***p<0.001.

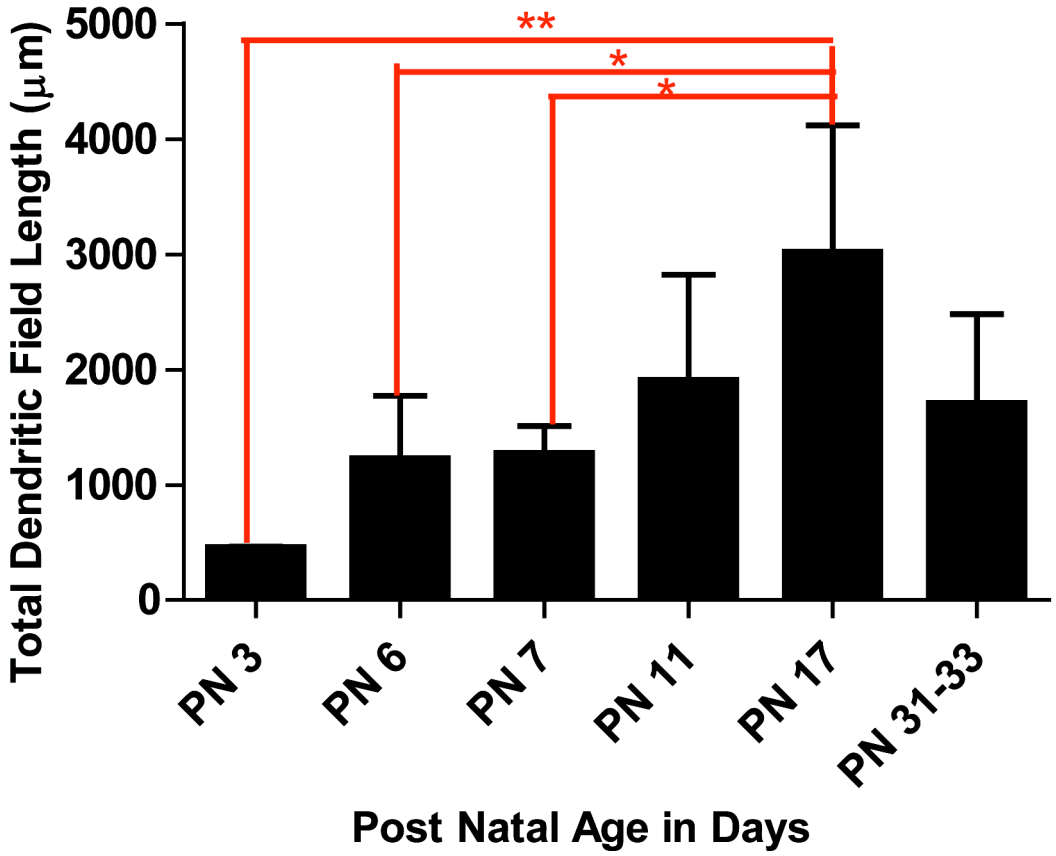

Figure 11: Plot of mean (± SD) M2 MRGC total dendritic field length (PN 3- PN 31/33). Asterisks indicate significance of Tukey analysis following ANOVA: *$p<0.05$; **$p<0.01$.

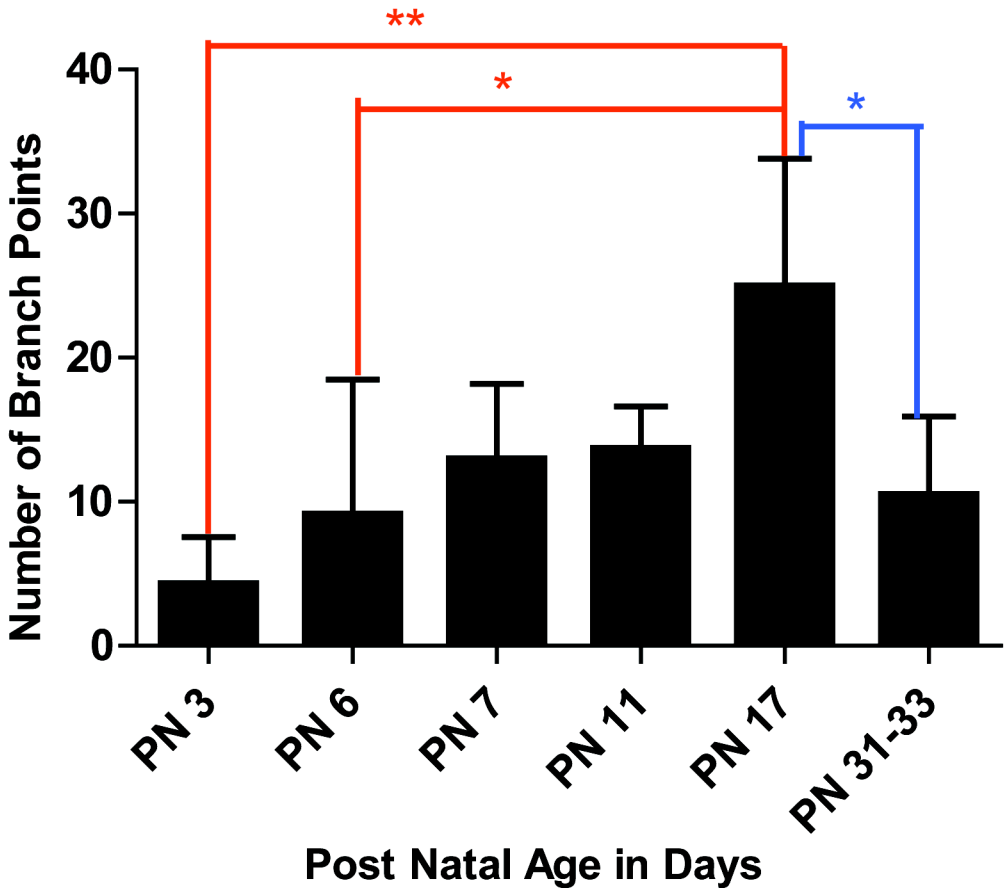

Figure 12: Plot of mean (± SD) number of dendritic branches of M2 MRGCs with respect to age (PN 3- PN 31/33). Asterisks indicate significance of Tukey analysis following ANOVA: *$p<0.05$; **$p<0.01$.

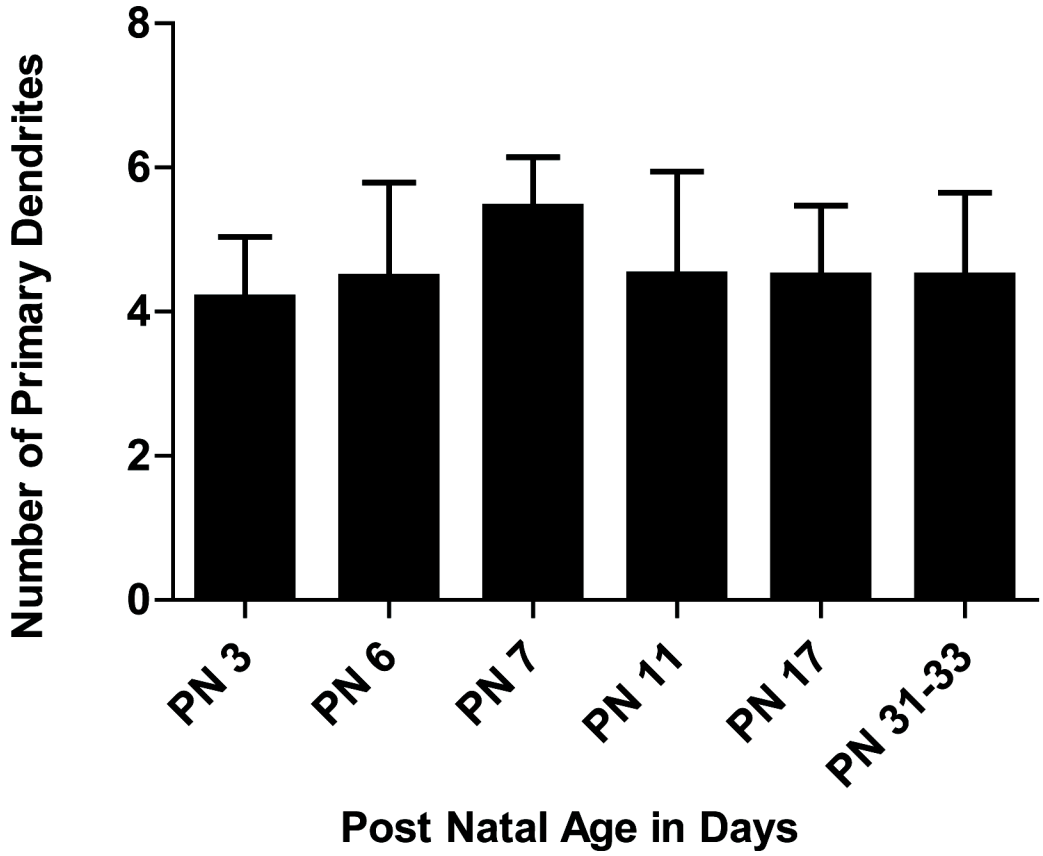

Figure 13: Plot of mean (± SD) number of primary dendrites of M2 MRGCs over the developmental period PN 3- PN 31/33.

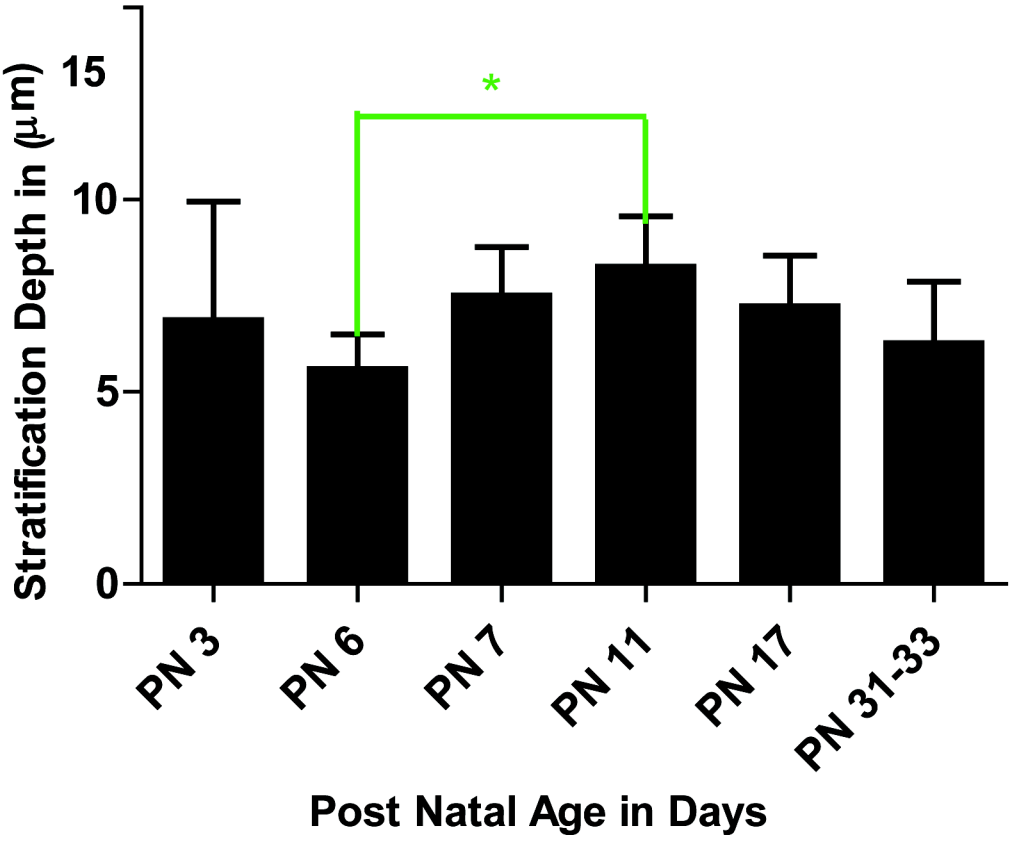

Figure 14: Mean (± SD) stratification depth of M2 MRGCs over the developmental period PN 3- PN 31-33. Asterisk indicates significance of Tukey analysis following ANOVA: *$p<0.05$.

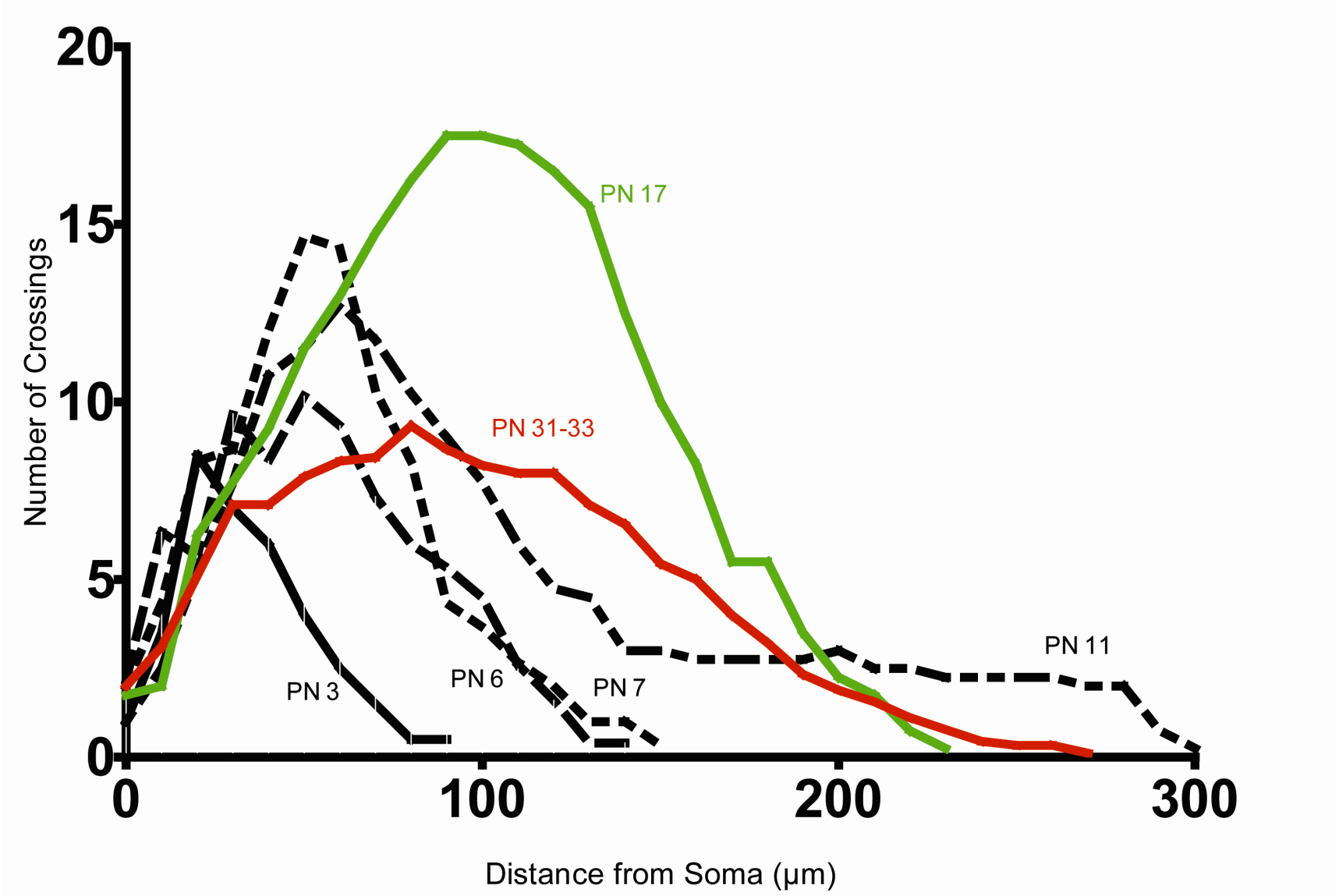
20
15
10
5
0
Number of Crossings
0
100
200
300
Distance from Soma (µm)
PN 17
PN 31-33
PN 11
PN 3
PN 6
PN 7

Figure 15: Plot of mean number of dendrites crossing at various eccentric distances from the soma (Sholl analysis) of M2 MRGCs at developmental periods PN 3 - PN 31/33.

CHAPTER 4: DISCUSSION

The vertebrate retina is an intricate, multilayered, central neuronal tissue that has long fascinated neuroscience researchers (including most notably, Ramon y Cajal, the father of modern neuroscience) and, naturally, has been a major focus of vision research. The retina can be extracted easily from the eye, is compact, thereby easily manipulated using a variety of preparations, and consists of the stereotypical patterns of cells. Therefore, this tissue has served as an ideal model for researchers attempting to gain a better understanding of the CNS. The retina is made up of many different populations of cells, many of which can be isolated (either physically or pharmacologically) in order to study their respective form and function.

Morphology has often been used as a method of classifying retinal neurons. Although cellular form is rarely a full predictor of function, it does impose limits and has proved as a useful foundation for physiological studies.

The potential for genetic manipulation has made the mouse retina a mainstay of retinal research, including the study of retinal ganglion cells (RGCs). One of the first studies to examine and quantify the different cell populations of the mouse retina was conducted by Jeon, Streotti and Masland (1998). Although they were able to identify larger cells within the GCL, via staining with ethidium homodimer, it was not clear which cells were RGCs (versus displaced amacrine cells) or to what extent different types of RGCs were stained. Subsequently, other methods were used to identify and classify RGCs such as intracellular injections of dye or tracer or by introducing DiI-coated tungsten particles into the retina via the gene gun method (Gan et al., 2000; Kong et al., 2005; Sun et al., 2002). With these methods it was often, but not always, possible to visualize the dendritic tree of labeled RGCs (Gan et al., 2000; Honig & Hume, 1986).

However, these approaches were limited by a high degree of technical difficulty, the indiscriminate distribution of dye within the retina and inability of the gene gun to penetrate beyond the most superficial cells (Sun et al., 2002).

Taking advantage of technology that permits the development of transgenic mice has allowed the directed, or more commonly fortuitous, expression of fluorescent protein in specific cell populations. For example, Huberman et al. (2009) were able to identify a subpopulation of on-off direction selective RGCs that expressed green fluorescent protein (GFP) under the control of the dopamine receptor 4 promoter. Similarly, in another study, (Kim et al., 2008) were able to identify another subpopulation of direction selective RGCs that responded to upward motion. In both instances, the morphology of the RGCs was distinct as the cells had an asymmetrical branch pattern that was consistent with their response to motion in a specific direction.

In this thesis I have identified a specific cell type, the M2 melanopsin-containing RGC (M2 MRGC), in the CLM-1 transgenic mouse line that expresses (though not uniquely) the fluorescent protein Clomeleon. Clomeleon is a fusion protein consisting of cyan and yellow fluorescent protein. Clomeleon expression was previously described in the retinas of CLM-1 animals, specifically in a type of bipolar cell, but it was also expressed by an abundance of neurons in the GCL . However, I am the first to identify that some Clomeleon-expressing GCL neurons are melanopsin-immunoreactive.

4.1. Characterization of the M2 MRGC

Melanopsin is the photopigment expressed in intrinsically photosensitive RGCs (ipRGCs). Only 1-3% of the RGCs in the rodent retina are ipRGCs. To date, as many as five subtypes MRGCs have been characterized, named M1, M2, M3, M4 and M5.

Melanopsin is found throughout MRGCs and, therefore, immunolabelling is found on the soma, the axon, and the dendrites of MRGCs. Consequently, melanopsin immunolabelling has often been used as a basis of morphological type identification (Berson et al., 2010; Dacey et al., 2005; Hattar et al., 2002; Tu et al., 2005), with results confirmed by other methods (dye or tracer injection, Ecker et al., 2010; Müller et al., 2010; Schmidt & Kofuji, 2009).

Several studies have been undertaken to establish the morphological properties of the five types of MRGCs (see Tables 2-6). Most is known about the first three types of MRGCs, M1-M3, with less evidence concerning the more recently described latter two types (M4 and M5). The reason for this is that a commonly used melanopsin antibody (UF006; rabbit polyclonal raised again 15 most N-terminal amino acids of mouse melanopsin; (Provencio, Rollag, & Castrucci, 2002) only labels M1-M3 MRGCs (Ecker et al., 2010). M1 MRGCs have relatively (compared to other MRGCs) small somas and large, sparsely branched dendritic arbors (Berson et al., 2010). Their dendrites are narrowly (mono) stratified and are localized in the outer margin (sublamina a) of the IPL (Berson et al., 2010; S. Hattar et al., 2006). M2 MRGCs, on the other hand, are located in the inner part (sublamina b) of the IPL (Berson et al., 2010; Hattar et al., 2006). Their soma sizes are larger, and they have monostratified dendritic fields that are larger than those of M1 MRGCs (Berson et al., 2010). M3 MRGCs are less common but are unique among MRGCs by being bistratified, with dendrites in both sublamina a and b of the IPL (Berson et al., 2010). M4 MRGCs are monostratified (sublamina b), have a large soma and a large, radiate dendritic arbour (Ecker et al., 2010). Although M4 cells are similar in many ways to M2 MRGCs, they are distinguished from M2 MRGCs on the basis of total dendritic length and the number of dendritic branch points. M5 MRGCs are compact and

have a highly branched dendritic arbor that extends broadly throughout sublamina b of the IPL (Ecker et al., 2010).

I propose that the Clomeleon-expressing, melanopsin-immunoreactive (CM+/M-IR) RGCs discovered in the CLM-1 mouse GCL corresponds to the M2 MRGC type. First, the CM+/M-IR RGCs were all monostratified with processes ramifying in sublamina b of the IPL. Although consistently observed qualitatively, this was also quantified by measuring the stratification depth, the distance from the soma to the most distal dendrites within the IPL, which was found to be 6 µm ± 2 µm (mean ± SD, n=18). Considering that the average thickness of the adult mouse IPL is 39 µm ± 10 µm (Coombs et al., 2007), this clearly puts the dendrites of the CM+/M-IR RGCs in sublamina b. This means the CM+/M-IR RGC has to be either an M2 or M4 MRGC. That it is the M2 type is established by 3 pieces of evidence. First, the antibody we used (UF006, see above) reportedly does not label the M4 MRGC (Ecker et al., 2010). Furthermore, total dendritic length of the CM+/M-IR RGCs (1,454 µm ± 785 µm; mean ± SD, n=9) was consistent with the measurement by Ecker et al. (2010) for M2 MRGCs (1,553 µm ± 428 µm, n=8) but not M4 MRGCs (4,584 µm ± 1465 µm, n=17). Similarly, the number of dendritic branch points (11 ± 5) was similar to values for M2 MRGCs (14 ± 4) but not M4 MRGCs (38 ± 10) cells. These two parameters are important because they are the only morphological features that clearly distinguish M2 and M4 MRGCs (Ecker et al., 2010).

The morphological parameters of the CM+/M-IR RGC, which I will refer to now as the M2 MRGC, is also similar to the characteristics of other published reports of M2 MRGCs (Berson et al., 2010; Müller et al., 2010; Schmidt & Kofuji, 2009) as well RGCs described previously but now thought to be (or to contain) M2 MRGCs (RG_{A1} type of

Sun et al., 2002 M6 ON cells of Coombs et al., 2006, the G1 cells of Völgyi et al., 2009; see Table 12). However, most of the measured parameters are not, in fact, specifically descriptive for M2 MRGCs. One study (Schmidt & Kofuji, 2009) reported that the total dendritic length of M2 MRGCs was considerably larger (4,131 μm ± 988 μm, n=13) than that reported by Ecker et al. (2010). However, this discrepancy is probably due to the fact that Schmidt & Kofuji (2010) did not recognize existence of M4 MRGCs and, therefore, many of the cells they identified as M2 MRGCs could, in fact, be M4 MRGCs.

The identification of the M2 MRGC in the CLM-1 mouse provides a means to identify this cell type during postnatal development. I studied the morphology of M2 MRGCs in animals as young as PN 3 and, as described above, as old as adult (PN 31-33). A focus of this work was postnatal development prior to eye opening (around PN 13) to determine if, compared to conventional RGCs, the intrinsic photosensitivity of MRGCs influences M2 MRGC morphology prior to the establishment of synaptic input from bipolar cells. An underlying assumption of this work is that melanopsin-immunoreactive, Clomeleon-expressing cells are M2 cells at different developmental time points.

4.2. Development of M2 RGCs

The pattern of morphological postnatal development of mouse RGCs depends on which parameter is being investigated (Coombs et al., 2007; Qu & Myhr, 2011) and very likely the specific cell type involved (Ren et al., 2010). Nonetheless, three consistent patterns have emerged, with some parameters essentially fixed at birth, others showing consistent changes from birth to adult, and others showing an initial period of growth (from birth to PN 10 – PN 20) followed by a retraction phase. From the perspective of cell type, and examining just one parameter (dendritic field size), Ren et al. (2010)

reported similar patterns, with most "conventional" mouse RGCs showing initial growth up to PN 13 followed by a retraction phase, the distinctively large "α" RGCs showing growth up to P13 but without a retraction phase and, lastly, an identifiable group of direction-selective RGCs that showed continued growth from birth through to adult.

I studied 6 morphological parameters of the M2 MRGC over the postnatal period P3 to adult. Similar to Coombs et al. (2007) and Qu & Myhr (2011) three different patterns of development were noted, depending on parameter. The number of primary dendrites and dendritic stratification were consistent from birth to adult. Dendritic field size showed an increase, peaking at the adult, but only starting at PN 17. Most of the parameters I measured (soma size, total dendritic length, number of branch points and Sholl analysis) showed an increase that peaked at PN 17 followed by a decrease in the adult. Although I observed three different patterns of postnatal morphological development for the M2 MRGC, my results, with respect to each parameter, are not completely consistent with the more general descriptions reported by Coombs et al. (2007) and Qu & Myhr (2011). Therefore, for each parameter, below I will contrast the similarities and differences with the previous studies of Coombs et al. (2007) and Qu & Myhr (2011) and compare and contrast my results with other studies of M2 MRGCs.

4.2.1Dendritic field size

As reported above, I found that the dendritic field size of M2 RGCs increased starting at PN 17, expanding further in the adult. This result is similar with the results of Coombs et al. (2007) where dendritic field area increased steadily from birth to adult. A difference is that I did not detect a statistically significant increase in dendritic field size until PN 17. Qu & Myhr (2011) also found a delayed expansion (starting at PN 8) of

dendritic field area but reported a contraction phase after PN 16-20. Dendritic field size was the only parameter assessed by Ren et al. (2010) and a pattern similar to what we observed for M2 MRGCs (greatest expansion later during PN development but without subsequent retraction) was evident in α-RGCs. One defining characteristic of α-RGCs is their large size, in particular the soma. Given that M2 RGCs have relatively large somata, it is likely that they constitute a portion of cells that would be classified as α-RGCs and, therefore, it is reasonable that their developmental pattern would be similar to α RGCs.

4.2.2. Soma area/radius, total dendritic field length and number of branch points

I found the following parameters to have relatively similar growth trends: soma area/radius, total dendritic field length (TDFL) and the number of branch points. Measurements of each of these parameters showed little initial change (PN 3-PN 7), then rapid growth (PN 7- PN 17) and subsequently a contraction phase (PN 17- adult). With respect to TDFL and the number of branch points, my results are consistent with the studies of Coombs et al. (2007) and Qu & Myhr (2011). However, with respect to soma size (area or radius) my results are different in that both Coombs et al. (2007) and Qu & Myhr (2011) reported a steady increase in soma size from birth to adult. A similar soma area growth trend was also reported by Diao et.al (2004). In their study they found that the soma area of randomly (gene gun) labeled mouse RGCs increased gradually over time, from PN 0 to adult. One limitation of this latter study was that animals between PN 13 and adult were not examined; this could be important as, for example, I found that the peak of soma area expansion was at PN 17.

The TDFL growth pattern I observed in M2 MGCs was different from that reported for M2 MRGC by Schmidt et al. (2008). They noted a steady increase of TDFL

over the period PN 0 - PN 24, reaching a maximum of 3,337 µm ± 1,480 µm (mean ± SD, n=17). Recall that the adult value for TDFL determined by this group (Schmidt & Kofuji, 2009) was 4,131 µm ± 988 µm (n=13). From this, it one would conclude continued growth of TDFL from birth the adult. However, also recall that this group did not distinguish between M2 and M4 MRGC types, making it difficult to determine to what extent the mean values for M2 MRGCs are inflated by data from M4 MRGCs.

4.2.3. Number of primary dendrites and stratification

The previously discussed parameters demonstrate that some of the morphological parameters of M2 MRGCs change with respect to postnatal age. There were also parameters, specifically the number of primary dendrites and extent of stratification in the IPL, which were not affected by age. The absence of a change in the number of primary dendrites I found is consistent with the result for RGCs in general reported by Coombs et al. (2007), which is the only other study that I am aware of that considered this parameter.

I found little evidence of change in stratification of M2 MRGCs, with mean values of stratification depth significantly different only between PN 6 and PN 11. The absence of a change in stratification in M2 MRGCs was a surprising result, as several studies, including studies of MRGCs, have reported alterations of dendritic stratification during development.

Coombs et al. (2007) found that RGC dendrites are initially (PN 1) ramified across the whole of the IPL that, at this age, is very thin (9.9 µm ± 2.1 µm, mean ± SD, n=17). There is a very rapid refinement of dendrites such that by PN 4-PN 5 they are about half way to attaining their adult position within the IPL and, by PN 10, are at the adult level. To some extent, my data for M2 MRGCs is consistent with such pattern, in

that a difference was noted between PN 6 and PN 11. A reason I may not have observed a change in stratification of M2 MRGCs at younger ages is that my earliest comparisons were made at PN 3 and PN 6. Studies of M2 MRGCs at PN 0-PN 2 might reveal alterations in dendritic stratification. Nonetheless, based on the results of Coombs et al. (2007), a difference between PN 3 and PN6 and PN 11 might have been expected. Another issue is the change in IPL thickness during development, also reported by Coombs et al. (2007). This means that even with little change in stratification depth, the portion of the IPL occupied by the M2 MRGCs would decrease.

Stratification is one feature that has been studied previously in MRGCs during postnatal development (Schmidt et al., 2008). MRGCs (of unknown type) were found to be monostratified even at early developmental periods (PN 5 or perhaps even as early as PN 2). Although they used choline acetyl transferase (ChAT) labeling, a marker of ON and OFF cholinergic amacrine cells, including their neurites in sublamina b and a of the IPL, respectively, at these young ages it was difficult to be certain about the position of the different sublaminas. Nonetheless, that MRGCs might be monostratified early on during development would be consistent with my observation of little change in stratification depth from PN 3 to adult.

4.2.4. Sholl analysis

Sholl analysis is a measure of dendritic complexity that assesses the number of dendrites that cross an expanding series of concentric rings placed around the cell. One metric derived from this analysis is the peak number of dendritic crossings. My application of Sholl analysis to the M2 MRGC at different postnatal ages indicated a pattern, seen in three other parameters (soma area, total dendritic length, number of

branch points) where there is an increase up to PN 17 followed by a retraction phase in the adult. To the best of my knowledge, Sholl analysis has not been applied to the study of mouse RGC (let alone MRGC) development and, therefore, it is not possible to directly compare my results to any published reports.

4.3. Tiling

Four out of the six parameters I studied (soma area, total dendritic length, number of branch points and Sholl analysis) demonstrated a developmental trend of limited growth (PN 3-PN 6) followed by rapid growth (PN 7- PN 17) and a decrease (PN 17 – adult). Although the size of the dendritic field increased from PN 17 to adult, the complexity of the dendritic arbor was reduced. What might be the basis for such a pattern of dendritic development?

As described by Sernagor et al. (2001), one explanation is that during development RGC dendrites undergo a dynamic rearrangement. The number of RGC dendrites initially increases then decreases with maturation the result of "pruning" . A causative factor explaining this pruning process is a phenomenon known as *tiling*.

Tiling is a process that refers to the mosaic growth pattern of dendrites of RGCs. This phenomenon was first introduced to explain the organization of α-RGCs of the cat retina (Wassle, Peichl, & Boycott, 1981) . The mosaic means that RGCs will cover the entire retina with their dendritic arbors, but limited so that the entire visual space is 'seen' by at least one RGC . Interaction that affect dendritic growth occur in two forms: the first is a "repel-like" mode, and the second a "seek or retract" mode. In the first mode, those cells that are of the same or similar type repel one another. Instead of overlapping their dendritic arbors, they will stop expanding. In the second mode, some dendrites will form

synapses with other neurons (bipolar cells and amacrine cells), others will not. Those that do not will retract.

I found a number of parameters of M2 MRGCs where there was a progressive decrease from PN17 to adult, although dendritic field size was not one of them. Thus, it could be that the M2 MRGCs undergo some form of maturation associated with tiling (i.e complexity of the dendritic arbor) without changing the overall diameter of the dendritic field.

4.4. Extrinsic influences on M2 RGC development

A key feature of postnatal RGC development is the formation of synapses with bipolar cells and the stratification and maturation of the dendritic arbour shortly after eye opening (Xu & Tian, 2007). It is a reasonable hypothesis, though largely untested, that the changes in RGC development that happen near the time of eye opening, including those I observed with respect to M2 MRGC morphology, are due to light-induced signalling from bipolar cells to RGCs. Although there is some question about to what extent RGC morphological development depends on the spontaneous or light-induced responses of bipolar cells (Diao et al., 2004), there is compelling evidence that light deprivation can prevent appropriate dendritic stratification, particularly within sublamina a of the IPL (Xu & Tian, 2007). This suggests, therefore, that the emergence of light-sensitive bipolar cells after eye opening has some influence on aspects of RGC development.

That MRGCs are intrinsically photosensitive, even at birth (Schmidt et al., 2008), raises the possibility that the light responses of these cells have some impact on their development, including morphology. However, my study of M2 MRGCs did not reveal anything remarkably different about the morphological development of M2 MRGCs with

most of the changes observed similar to features observed for other types of RGCs and, as described above, possibly influenced by bipolar cell activity after eye opening.

4.5. Limitations

Some of the morphological parameters for M2 RGCs reported here, in particular measurements of dendritic field size and total dendritic length, depend on the complete labeling of dendrites by the melanopsin antibody. As described previously, the expression of melanopsin throughout the cell, including the soma, axon and dendrites, makes it at least plausible that immunolabelling can be used to reveal the dendritic morphology (Berson et al., 2010; Dacey et al., 2005; Hattar et al., 2002; Tu et al., 2005). However, it is possible that certain parameters could have been underestimated if there was incomplete labeling of the finest, most distal, dendrites. The best evidence I can offer that this is not the case is that while my measurements of mean dendritic field was not significantly different from other reported values for those MRGCs with the largest dendritic field size (M2 and M4 RGCs, see Tables 3,5, 7). Although a superior method would be to undertake intracellular injection of M2 RGCs at different developmental time points with dye or tracer, the CLM-1 mouse is not ideal for this purpose, as a wide variety of cells types are Clomeleon expressing in the GCL. That is, the only way to identify the M2 RGC in this transgenic mouse line is to perform melanopsin immunohistochemistry using fixed tissue (which cannot be used for intracellular dye or tracer experiments). On the other hand, because the somata of the M2 RGC is quite large, likely identified in the past as an α-cell, it might be possible to inject it with dye or tracer by targeting only the largest cells, and then confirming the identity of the cell using melanopsin immunohistochemistry.

Another assumption held during this study was that cells sampled from the same retina or animal were independent. Although such an assumption is common in studies of RGCs (Schmidt & Kofuji, 2009; Coombs et al., 2007), if not accepted, this would substantially reduce an already modest sample size. One solution would be to establish sample size as the number of animals studied, but combine same age groups together. For example, PN 6 and 7 could be combined (to yield n = 8 animals), PN 7 and 11 could be combined (n = 9 animals), and PN 13 (not included in the current data set) could be combined with PN 17 (n= 5 animals).

4.6. Conclusion and future directions

An intriguing aspect of RCGs is that they are intrinsically photosensitive from birth. I had wanted to determine if this quality had an impact on the developmental morphology of these cells. By identifying and characterizing one melanopsin cell type, the M2 MRGC, I found that its morphological development was consistent with published descriptions of the development of conventional RGCs. Thus, under normal light and dark conditions there does not seem to be gross changes in M2 MRGC morphological development. Future studies could include examining the morphology of M2 MRGCs and their development under abnormal light conditions, such as light deprivation. Interestingly, targeted replacement or deletion of the melanopsin gene (Opn $4^{-/-}$) apparently does not affect the morphology of adult MRGCs (Hatori et al., 2008; Lucas et al., 2003). While this is consistent with the conclusion that the intrinsic photosensitivity of MRGCs (including the M2 MRGC) does not affect postnatal development, in fact the extent of the morphological characterization of MRGCs in melanopsin knock-out mice was rather limited. For example, these studies did not take

into consideration (or were not yet aware) of the different types of MRGCs. Therefore, another approach that could be taken would be to study in greater detail the morphology of MRGCs, in adult and during development, in melanopsin knock-out mice and, in particular, taking into account the most recent information about MRGC subtypes.

Table: 2

Reference	Cell	Age	Branching pattern	Soma size (μm)	Dendritic Field (μm)	Stratification % of IPL or identified layer
Müller et al., 2010	M1	>3 Months	-	16.7 ± 3.6	377± 81	Sublamina a
Schmidt and Kofuji, 2009	M1	Adult	Less branched than M2	17.0 ± 0.4	313.6 ± 17.3	OFF sublamina
Ecker et al., 2010	M1	PN 2-4 months	sparsely	15.6 ± 2.4	350 ± 87	outer (OFF) sublamina
Berson Castrucci, & Provencio, 2010	M1	Adult		13.0 ± 1.4	275 ± 82	outer (OFF) plexus
Coombs et.al, 2006	M6 OFF	Adult	Large, sparse	125-200		OFF

Characteristics of M1 MRGCs and related RGC types.

Table: 3

Reference	Cell	Age	Branching pattern	Soma size (μm)	Dendritic Field (μm)	Stratification % IPL or identified layer
Müller, et al., 2010	M2	>3 Months	-	18.6 ± 3.8	403 ± 109	Sublamina b
Schmidt and Kofuji, 2009	M2	Adult	Highly branched than M1	21.8 ± 0.8	422.9 ± 23.5	ON
Ecker et al., 2010	M2	PN 2-4 months	Orderly, regular branching	17.4 ± 1.7	324 ± 30	ON
Berson Castrucci, & Provencio, 2010	M2	Adult	Regular branching dendrites	14.8 ± 1.5	314 ± 76	67-83
Coombs et al,. 2006	M6 ON	Adult		14-17	300-415	92-97

Characteristics of M2 MRGCs and related RGC types.

Table: 4

Reference	Cell	Age	Branching pattern	Soma size (μm)	Dendritic Field (μm)	Stratification % of IPL or identified layer
Müller, et al., 2010	M3	>3 Months	bistratified	16.7 ± 3.2	449 ± 60	Sublamina a and b
Ecker et al., 2010	M3	PN 2-4 months	bistratified	15.7 ± 2.2	bistratified	outer (OFF) sublamina and inner (ON) lamina
Berson Castrucci, & Provencio, 2010	M3	Adult	Bistratified	14.5	Large similar to M1 and M2	outer (OFF) plexus and inner (ON) plexus
Coombs et al,. 2006	G 12	Adult	Bistratified	14.3 ± 2.5	201.2 ± 42.3	32.8 ± 11.7 (OFF) 66.7 ± 8.1 (ON)

Characteristics of M3 MRGCs and related RGC types.

Table:5

Reference	Cell	Age	Branching pattern	Soma size (μm)	Dendritic Field (μm)	Stratification % IPL or identified layer
Ecker et al., 2010	M4	PN 2-4 months	Large radiate dendritic arbour	17.1-22.3	302-444	Inner (ON) sublamina
Coombs et al., 2006	M6	Adult		14-17	300-415	92-97

Characteristics of M4 MRGCs and related RGC types.

Table: 6

Reference	Cell	Age	Branching pattern	Soma size (μm)	Dendritic Field (μm)	Stratification % IPL or identified layer
Ecker et al., 2010	M5	PN 2-4 months	Bushy, small and compact	16.4± 4	149-217	Inner (ON) sublamina
Coombs et al., 2006	M	Adult				

Characteristics of M5 MRGCs and related RGC types.

Table: 7

Reference	Age	Cell	Soma Area	Soma diameter (um) (mean ± sd)	Dendritic Field (um) (mean ± sd)	Total Dendritic Length (um) (mean ± sd)	Stratification in % IPL / identified layer / or in um
Muller et al., 2010	>2 months old	M2	-	18.6 ± 3.8	403 ± 109		Sublamina b
Schmidt and Kofuji, 2009	Adult	M2	_	21.8 ± 0.8	422.9± 23.5	4131.4 ± 273.7	ON
Ecker et al., 2010	PN 2-4 months of age	M2	-	17.4± 1.7	324± 30	1553 ± 428	ON
Ecker et al., 2010	PN 2-4 months of age	M4	-	17.1-22.3	353 ± 73	4584± 1465	ON
Berson, Castrucci & Provencio, 2010	Adult		-	14.8 ± 1.5	314 ± 76		67-83%
Coombs et al., 2006	Adult	M6 ON		14-17	300-415		92-97%
Kong et al., 2005	Cluster 11		-	-	380	-	76.00%
Volgyi et al., 2009	PN 30-90 Days	G1 G2		20.3 ± 3.4 17.6 ± 2.9	245 ± 30 200 ± 42		78± 8.4 % 73± 8.1%
Sun et al., 2002	Adult	RGA1		22± 4	318 ± 74		73 ± 9 %
		RGC 3		15± 2	296 ± 107		68± 16%
THIS THESIS	**PN 30-33**	**M2**	**285 ± 130**	**19 ± 4**	**268 ± 66**	**1454 ± 785**	**6.6 ± 1.44**

Comparison of M2 and M4 MRGCs and related RGC types.

References

Badea, T., & Nathans, J. (2004). Quantitative analysis of neuronal morphologies in the mouse retina visualized by using a genetically directed reporter. *Journal of Comparative Neurology, 480*(4), 331-351.

Bailes, H., & Lucas, R. (2010). Melanopsin and inner retinal photoreception. *Cellular and Molecular Life Sciences, 67*(1), 99-111.

Baldridge, W. H., Wang, X., Forsythe, M., Berglund, K., Augustine, G., & Muller Pérez de Sevilla, L. (2012). Displaced ganglion cells in the clomeleon (CLM-1) mouse retina. [Abstract]. *Investigative Ophthalmology & Visual Science 2012; 53:ARVO E-Abstract 1953., 53* 1953.

Barlow, H. B., Hill, R. M., & Levick, W. R. (1964). Retinal ganglion cells responding selectively to direction and speed to image motion in the rabbit. *Journal of Physiology, 173*, 377-407.

Berglund, K., Schleich, W., Krieger, P., Loo, L., Wang, D., Cant, N., Feng, G., Augustine, G., & Kuner, T. (2006). Imaging synaptic inhibition in transgenic mice expressing the chloride indicator, clomeleon. *Brain Cell Biology, 35*(4-6), 207-228.

Berson, D., Castrucci, A., & Provencio, I. (2010). Morphology and mosaics of melanopsin-expressing retinal ganglion cell types in mice. *Journal of Comparative Neurology, 518*(13), 2405-2422.

Berson, D., Dunn, F., & Takao, M. (2002). Phototransduction by retinal ganglion cells that set the circadian clock. *Science, 295*(5557), 1070-1073.

Boycott, B. B., & Wassle, H. (1974). The morphological types of ganglion cells of the domestic cat's retina *Journal of Physiology, 240*, 397-419.

Cleland, B. G., & Levick, W. R. (1974). Brisk and sluggish concentrically organized ganglion cells in the cat's retina. *Journal of Physiology, 240*, 421-456.

Coombs, J., Van Der List, D., & Chalupa, L. (2007). Morphological properties of mouse retinal ganglion cells during postnatal development. *Journal of Comparative Neurology, 503*(6), 803-814.

Cugell-Enroth, C., & Robson, J. G. (1966). The contrast sensitivity of retinal ganglion cells of the cat. *Journal of Physiology, 187*, 517-552.

Dacey, D., Liao, H., Peterson, B., Robinson, F., Smith, V., Pokorny, J., Yau, K.-W., & Gamlin, P. (2005). Melanopsin-expressing ganglion cells in primate retina signal colour and irradiance and project to the LGN. *Nature, 433*(7027), 749-754.

Diao, L., Sun, W., Deng, Q., & He, S. (2004). Development of the mouse retina: Emerging morphological diversity of the ganglion cells. *Journal of Neurobiology, 61*(2), 236-249.

Do, M. T. H., & Yau, K. (2010). Intrinsically photosensitive retinal ganglion cells. *Physiological Reviews, 90*(4), 1547-1581.

Dowling, J. E. (2012). *The retina an approachable part of the brain*. Cambridge: Belknap press of Harvard University Press.

Ecker, J., Dumitrescu, O., Wong, K., Alam, N., Chen, S., LeGates, T., . . . Hattar, S. (2010). Melanopsin-expressing retinal ganglion-cell photoreceptors: Cellular diversity and role in pattern vision. *Neuron, 67*(1), 49-60.

Galli Resta, L., Leone, P., Bottari, D., Ensini, M., Rigosi, E., & Novelli, E. (2008). The genesis of retinal architecture: An emerging role for mechanical interactions? *Progress in Retinal and Eye Research, 27*(3), 260-283.

Gan, W. B., Grutzendler, J., Wong, W. T., Wong, R. O., & Lichtman, J. W. (2000). Multicolor "DiOlistic" labeling of the nervous system using lipophilic dye combinations. *Neuron, 27*(2), 219-225.

Goldberg, J. (2008). Axon growth and regeneration of retinal ganglion cells. In L. M. Chalupa, & R. W. Williams (Eds.), *Eye, retina, amd visual system of the mouse* (pp. 401). Cambridge: The MIT Press.

Goldberg, J., Espinosa, J., Xu, Y., Davidson, N., Kovacs, G. T. A., & Barres, B. (2002). Retinal ganglion cells do not extend axons by default: Promotion by neurotrophic signaling and electrical activity. *Neuron, 33*(5), 689-702.

Gooley, J. J., Lu, J., Chou, T. C., Scammell, T. E., & Saper, C. B. (2001). Melanopsin in cells of origin of the retinohypothalamic tract. *Nature Neuroscience, 4*(12), 1165-1165.

Hannibal, J., Hindersson, P., Knudsen, S., Georg, B., & Fahrenkrug, J. (2002). The photopigment melanopsin is exclusively present in pituitary adenylate cyclase-activating polypeptide-containing retinal ganglion cells of the retinohypothalamic tract. *The Journal of Neuroscience, 22*(1), RC191-RC191.

Hatori, M., Le, H., Vollmers, C., Keding, S., Tanaka, N., Schmedt, C., Jegla, P, & Panda, S. (2008). Inducible ablation of melanopsin-expressing retinal ganglion cells reveals their central role in non-image forming visual responses. *PLoS ONE, 3*(6), e2451-e2451.

Hattar, S., Liao, H. W., Takao, M., Berson, D. M., & Yau, K. W. (2002). Melanopsin-containing retinal ganglion cells: Architecture, projections, and intrinsic photosensitivity. *Science, 295*(5557), 1065-1070.

Hattar, S., Lucas, R. J., Mrosovsky, N., Thompson, S., Douglas, R. H., Hankins, M. W., Lem, J., Biel, M., Hofmann, F., Foster, R., & Yau, K. (2003). Melanopsin and rod-cone photoreceptive systems account for all major accessory visual functions in mice. *Nature, 424*(6944), 76-81.

Hattar, S., Kumar, M., Park, A., Tong, P., Tung, J., Yau, K., & Berson, D. (2006). Central projections of melanopsin-expressing retinal ganglion cells in the mouse. *Journal of Comparative Neurology, 497*(3), 326-349.

Haverkamp, S., Wassle, H., Duebel, J., Kuner, T., Augustine, G., Feng, G., & Euler, T. (2005). The primordial, blue-cone color system of the mouse retina. *The Journal of Neuroscience, 25*(22), 5438-5445.

Honig, M. G., & Hume, R. I. (1986). Fluorescent carbocyanine dyes allow living neurons of identified origin to be studied in long-term cultures. *The Journal of Cell Biology, 103*(1), 171-187.

Huberman, A., Wei, W., Elstrott, J., Stafford, B., Feller, M., & Barres, B. (2009). Genetic identification of an on-off direction-selective retinal ganglion cell subtype reveals a layer-specific subcortical map of posterior motion. *Neuron, 62*(3), 327-334.

Jeon, C. J., Strettoi, E., & Masland, R. H. (1998). The major cell populations of the mouse retina. *The Journal of Neuroscience, 18*(21), 8936-8946.

Kandel, E. R., Schwartz, J. H., & Jessell, T. M. (2000). *Principles of neural science* (4th ed.). Toronto: McGraw Hill Companies Incorporated.

Kim, I., Zhang, Y., Yamagata, M., Meister, M., & Sanes, J. (2008). Molecular identification of a retinal cell type that responds to upward motion. *Nature, 452*(7186), 478-482.

Kong, J., Fish, D., Rockhill, R., & Masland, R. (2005). Diversity of ganglion cells in the mouse retina: Unsupervised morphological classification and its limits. *Journal of Comparative Neurology, 489*(3), 293-310.

Leamey, C. A., Protti, D. A., & Bogdan, D. (2008). Comparative survey of the mammalian visual system with reference to the mouse. In L. M. Chalupa, & R. W. Williams (Eds.), *Eye, retina, and visual system of the mouse* (pp. 35)

Levick, W. R. (1967). Receptive fields and trigger features of ganglion cells in the visual streak of the rabbit's retina. *Journal of Physiology, 188*, 285-307.

Lucas, R. J., Hattar, S., Takao, M., Berson, D. M., Foster, R. G., & Yau, K. (2003). Diminished pupillary light reflex at high irradiances in melanopsin-knockout mice. *Science, 299*(5604), 245-247.

Lyubarsky, A. L., Falsini, B., Pennesi, M. E., Valentini, P., & Pugh, E. N. J. R. (1999). UV- and midwave-sensitive cone-driven retinal responses of the mouse: A possible phenotype for coexpression of cone photopigments. *Journal of Neuroscience, 19*, 442-455.

McNeill, D., Sheely, C., Ecker, J., Badea, T., Morhardt, D., Guido, W., & Hattar, S. (2011). Development of melanopsin-based irradiance detecting circuitry. *Neural Development, 6*, 8-8.

Müller, L. P. d. S., Do, M. T. H., Yau, K., He, S., & Baldridge, W. (2010). Tracer coupling of intrinsically photosensitive retinal ganglion cells to amacrine cells in the mouse retina. *Journal of Comparative Neurology, 518*(23), 4813-4824.

Napier, H. R. L., & Link, B. A. (2009). Retinal development: An overview. In G. Lemke (Ed.), *Developmental neurobiology* (pp. 251). Milwaukee: Elsevier.

Nikonov, S., Kholodenko, R., Lem, J., & Pugh, E. (2006). Physiological features of the S- and M-cone photoreceptors of wild-type mice from single-cell recordings. *The Journal of General Physiology, 127*(4), 359-374.

Panda, S., Sato, T. K., Castrucci, A. M., Rollag, M. D., Degrip, W. J., Hogenesch, J. B., Provencio, I., & Kay, S. A. (2002). Melanopsin (Opn4) requirement for normal light-induced circadian phase shifting. *Science, 298*, 2213-2216.

Peichl, L., Sandmann, D., & Boycott, B. B. (1998). Comparative anatomy and function of mammalian horizontal cells. In L. M. Chalupa, & B. L. Finlay (Eds.), *Development and organization of the retina* (). New York: Plenum Press.

Provencio, I., Jiang, G., DeGrip, W. J., Hayes, W. P., & Rollag, M. D. (1998). Melanopsin: An opsin in melanophores, brain and eye. *PNAS Proceedings of the National Academy of Sciences, 95*, 340-345.

Provencio, I., Rollag, M., & Castrucci, A. (2002). Photoreceptive net in the mammalian retina. this mesh of cells may explain how some blind mice can still tell day from night. *Nature, 415*(6871), 493-493.

Qu, J., & Myhr, K. (2011). The morphology and intrinsic excitability of developing mouse retinal ganglion cells. *PLoS ONE, 6*(7), e21777-e21777.

Remmington, L. A. (2005). *Clinical anatomy of the visual system* (Second ed.). St. Louis: Elsevier.

Ren, L., Liang, H., Diao, L., & He, S. (2010). Changing dendritic field size of mouse retinal ganglion cells in early postnatal development. *Developmental Neurobiology, 70*(6), 397-407.

Schmidt, T., Chen, S., & Hattar, S. (2011). Intrinsically photosensitive retinal ganglion cells: Many subtypes, diverse functions. *Trends in Neurosciences, 34*(11), 572-580.

Schmidt, T., Do, M. T. H., Dacey, D., Lucas, R., Hattar, S., & Matynia, A. (2011). Melanopsin-positive intrinsically photosensitive retinal ganglion cells: From form to function. *The Journal of Neuroscience, 31*(45), 16094-16101.

Schmidt, T., & Kofuji, P. (2009). Functional and morphological differences among intrinsically photosensitive retinal ganglion cells. *The Journal of Neuroscience, 29*(2), 476-482.

Schmidt, T., & Kofuji, P. (2010). Differential cone pathway influence on intrinsically photosensitive retinal ganglion cell subtypes. *The Journal of Neuroscience, 30*(48), 16262-16271.

Schmidt, T., Taniguchi, K., & Kofuji, P. (2008). Intrinsic and extrinsic light responses in melanopsin-expressing ganglion cells during mouse development. *Journal of Neurophysiology, 100*(1), 371-384.

Sernagor, E., Eglen, S. J., & Wong, R. O. (2001). Development of retinal ganglion cell structure and function. *Progress in Retinal and Eye Research, 20*(2), 139-174.

Stone, J., & Fukuda, Y. (1974). Properties of cat retinal ganglion cells: A comparison of W -cells with X- and Y- cells. *Journal of Neurophysiology, 37*(4), 722-748.

Sun, W., Li, N., & He, S. (2002). Large-scale morphological survey of mouse retinal ganglion cells. *Journal of Comparative Neurology, 451*(2), 115-126.

Trenholm, S., Johnson, K., Li, X., Smith, R., & Awatramani, G. (2011). Parallel mechanisms encode direction in the retina. *Neuron, 71*(4), 683-694.

Tu, D., Zhang, D., Demas, J., Slutsky, E., Provencio, I., Holy, T., & Van Gelder, R. (2005). Physiologic diversity and development of intrinsically photosensitive retinal ganglion cells. *Neuron, 48*(6), 987-999.

Volgyi, B., Chheda, S., & Bloomfield, S. (2009). Tracer coupling patterns of the ganglion cell subtypes in the mouse retina. *Journal of Comparative Neurology, 512*(5), 664-687.

Wingate, R. J. T., & Thompson, I. D. (1994). Targeting and activity -related dendritic modification in mammalian retinal ganglion cells. *Journal of Neuroscience, 14*, 6612-6637.

Wassle, H., Peichl, L., & Boycott, B. B. (1981). Dendritic territories of cat retinal ganglion cells. *Nature, 292*(5821), 344-345.

Xu, H., & Tian, N. (2007). Retinal ganglion cell dendrites undergo a visual activity-dependent redistribution after eye opening. *Journal of Comparative Neurology, 503*(2), 244-259.

Young, R. W. (1984). Cell death during differentiation of the retina in the mouse. *Journal of Comparative Neurology, 229*, 362-373.

Zhang, S. S., Fu, X. Y., & Barnstable, C. J. (2002). Tissue culture studies of retinal development. *Methods, 28*, 439-447.

Zhu,Y., Tu, D., Denner, D., Shane, T., Fitzgerald, C., & Van Gelder, R. (2007). Melanopsin-dependent persistence and photopotentiation of murine pupillary light responses. *Investigative Ophthalmology Visual Science, 48*(3), 1268-1275.